Tatsuo, H., Ono, N., Yanagi, Y., 2001. Morbilliviruses use signaling lymphocyte activation molecules (CD150) as cellular receptors. J. Virol. 75, 5842–5850.

Taylor, J., Pincus, S., Tartaglia, J., Richardson, C., Alkhatib, G., Briedis, D., Appel, M., Norton, E., Paoletti, E., 1991. Vaccinia virus recombinants expressing either the measles virus fusion or hemagglutinin glycoprotein protect dogs against canine distemper virus challenge. J. Virol. 65, 4263–4274.

Wang, L.-F., Collins, P.L., Fouchier, R.A.M., Kurath, G., Lamb, R.A., Randall, R.E., Rima, B.K., 2012. Family paramyxoviridae. In: King, A.M.Q., Adams, M.J., Carstens, E.B., Lefkowitz, E.J. (Eds.), Virus Taxonomy, 9th ed. Elsevier Academic Press, London, pp. 672–685.

von Messling, V., Svitek, N., Cattaneo, R., 2006. Receptor (SLAM [CD150]) recognition and the V protein sustain swift lymphocyte-based invasion of mucosal tissue and lymphatic organs by a morbillivirus. J. Virol. 80, 6084–6092.

Vaccine 29 (2011) 1863–1873

Contents lists available at ScienceDirect

Vaccine

journal homepage: www.elsevier.com/locate/vaccine

Elucidation of the full genetic information of Japanese rubella vaccines and the genetic changes associated with *in vitro* and *in vivo* vaccine virus phenotypes

Noriyuki Otsuki*, Hitoshi Abo, Toru Kubota, Yoshio Mori, Yukiko Umino, Kiyoko Okamoto, Makoto Takeda, Katsuhiro Komase

Department of Virology 3, National Institute of Infectious Diseases, Gakuen 4-7-1, Musashimurayama, Tokyo 208-0011, Japan

ARTICLE INFO

Article history:
Received 11 November 2010
Received in revised form 5 January 2011
Accepted 8 January 2011
Available online 18 January 2011

Keywords:
Rubella
Temperature-sensitive
Genome
Marker test
Attenuation

ABSTRACT

Rubella is a mild disease characterized by low-grade fever, and a morbilliform rash, but causes congenital defects in neonates born from mothers who suffered from rubella during the pregnancy. After many passages of wild-type rubella virus strains in various types of cultured cells, five live attenuated rubella vaccines were developed in Japan. An inability to elicit anti-rubella virus antibodies in experimentally infected animals was used as an *in vivo* marker phenotype of Japanese rubella vaccines. All Japanese rubella vaccine viruses exhibit a temperature-sensitive (ts) phenotype, and replicate very poorly at a high temperature. We determined the entire genome sequences of three Japanese rubella vaccines (Matsuba, TCRB19, and Matsuura), thereby completing the sequencing of all five Japanese rubella vaccines. In addition, the entire genome sequences of three vaccine progenitors were determined. Comparative nucleotide sequence analyses revealed mutations that were introduced into the genomes of the TO-336 and Matsuura vaccines during their production by laboratory passaging. Analyses involving cellular expression of viral P150 nonstructural protein-derived peptides revealed that the N1159S mutation conferred the ts phenotype on the TO-336 vaccine, and that reduced thermal stability of the P150 protease domain was a cause of the ts phenotype of some rubella vaccine viruses. The ts phenotype of vaccine viruses was not necessarily correlated with their inability to elicit humoral immune responses in animals. Therefore, the molecular mechanisms underlying the inability of these vaccines to elicit humoral responses in animals are more complicated than the previously considered mechanism involving the ts phenotype as the major cause.

1. Introduction

Rubella is a communicable and ordinarily mild disease that is characterized by low-grade fever, a short-lived morbilliform rash, and lymphadenopathy [1]. A German physician originally designated this disease 'German measles', since it resembles measles but is much less severe [1]. Arthralgia and arthritis are common complications of rubella, particularly in adolescent and adult females. Rubella has received much attention following a report that congenital cataracts were associated with rubella infection of mothers during pregnancy [2]. Subsequent studies indicated that sensorineural hearing loss and cardiovascular defects are also common in neonates born from mothers who suffered from rubella, especially during the early phase of pregnancy [1].

Rubella virus (RuV) was first isolated in 1962 [3,4], and belongs to the genus *Rubivirus* in the family *Togaviridae*. After many passages of wild-type (wt) RuV strains in various types of cultured cells, live attenuated rubella vaccines were developed [1,5,6]. The first rubella vaccine was licensed in the United States in 1969 [7]. A total of nine vaccines (HPV-77, RA27/3, Cendehill, BRD-2, Matsuba, TCRB19, KRT, Matsuura, and TO-336) have been developed to date [1,7]. Among these, five vaccines were developed in Japan [6].

An increased growth rate in certain cultured cells has been used as an *in vitro* marker phenotype of Japanese rubella vaccines [6]. In addition, an inability to elicit anti-RuV antibodies in experimentally infected guinea pigs and rabbits has been used as an *in vivo* marker phenotype of Japanese rubella vaccines [6]. The Minimum Requirements for Biological Products (MRBP) announced by the Ministry of Health, Labour and Welfare, Japan, defines the *in vivo* phenotype as a marker phenotype of rubella vaccines [8,9]. All lots of commercially used Japanese rubella vaccines must receive a national test by the National Institute of Infectious Diseases, Japan, to verify this phenotype as a marker test [8,9]. Later, it was recognized that all Japanese rubella vaccines exhibit a temperature-sensitive (ts) phenotype, meaning that they replicate very poorly at a high temperature (39 °C), whereas wt strains can replicate well at that temperature [5]. Although understanding of the molecular bases for acquisition of these *in vitro* and *in vivo* vaccine virus pheno-

* Corresponding author. Tel.: +81 42 561 0771; fax: +81 42 562 8941.
E-mail address: otsuki@nih.go.jp (N. Otsuki).

0264-410X/$ – see front matter © 2011 Elsevier Ltd. All rights reserved.
doi:10.1016/j.vaccine.2011.01.016

types is crucial for quality control of vaccines, they have been poorly elucidated. In the present study, we performed various analyses to elucidate the genetic changes introduced into the genomes of rubella vaccines during passages under laboratory conditions and to show importance of these changes in determining the *in vitro* and *in vivo* vaccine virus phenotypes. Our data in the present study provide basic and solid information for the genetic changes of rubella vaccines as well as a novel insight into the understanding of molecular bases for the vaccine phenotypes.

2. Materials and methods

2.1. Cells and viruses

RK13 cells were cultured in Eagle's minimal essential medium (MEM) supplemented with 8% bovine serum. After infection with RuV, the cells were cultured in MEM containing 2% bovine serum. When transfected with plasmids, the cells were cultured in Dulbecco's modified Eagle's medium (DMEM) supplemented with 10% fetal bovine serum (FBS) and 0.1 mM non-essential amino acids.

Five licensed vaccines (KRT, Matsuba, TCRB19, TO-336, and Matsuura) were passaged once or twice in RK13 cells to obtain sufficient amounts of stocks. These vaccines were termed as KRT, Matsuba.vac, TCRB19, TO-336.vac, and Matsuura.vac, respectively, in the present study. Three wt strains, TO-336.GMK5, Matsuba.GMK3, and Matsuura.B3, isolated in Japan in the late 1960s were also passaged in RK13 cells once or twice to obtain sufficient amounts of virus stocks. The wt RVi/Hiroshima.JPN/01.03 strain isolated in Japan in 2003 was passaged four times in RK13 cells. A TO-336.vac-derived mutant clone that replicated well at a high temperature was generated as follows. RK13 cells were infected with TO-336.vac and incubated at 39 °C. A clone that replicated well at this temperature was plaque-purified and propagated in RK13 cells at 39 °C. The obtained clone was designated TO-336.rev.

2.2. Sequencing

Viral RNAs were extracted from each virus stock using a High Pure Viral RNA Kit (Roche Diagnostics GmbH, Mannheim, Germany) according to the manufacturer's instructions. Several cDNA fragments covering the entire virus genome were amplified using a One-step RT-PCR Kit (Qiagen KK, Tokyo, Japan). The primers used for amplification will be provided upon request. To determine the 5′ terminus of each viral genome, a 5′ RACE system (Invitrogen, Carlsbad, CA) was used. To amplify the 3′ terminus of the viral genome, an RNA PCR Kit (AMV) ver. 3.0 (Takara Bio, Shiga, Japan) was used with an oligo (dT) adaptor primer. The PCR products were purified using a QIAquick Gel Extraction Kit (Qiagen KK) and a QIAquick PCR Purification Kit (Qiagen KK). The nucleotide sequences of the purified PCR products were determined using a Big Dye Terminator v3.1 Cycle Sequencing Kit (Applied Biosystems, Foster City, CA) and a capillary sequencer. Some PCR products were cloned into the pCR2.1 vector (Invitrogen), and the nucleotide sequences of more than three clones were analyzed to determine a consensus sequence.

2.3. Sequence data analysis

The entire genome sequences of 13 RuV strains were used for comparisons. Data for seven RuV strains, Therien [10] (GenBank M15240), RA27/3 [11] (GenBank L78917), RVi/Matsue.JPN/68 [12] (GenBank AB222609), TO-336wt [13] (GenBank AB047330), TO-336.vac [13] (GenBank AB047329), M33 [11,14] (GenBank X72393 and X05259), and KRT [12] (GenBank AB222608) were reported previously. Corrected nucleotide sequence data were used for the Therien and M33 strains [11], rather than the original data (GenBank M15240, X72393, and X05259). The entire genome nucleotide sequences of six RuV strains, TCRB19, Matsuba.GMK3, Matsuura.B3, Matsuura.vac, TO-336.GMK5, and Matsuba.vac, were determined in the present study, and registered in GenBank under accession numbers AB588188, AB588189, AB588190, AB588191, AB588192, and AB588193, respectively. Analyses were performed using the GENETYX-MAC ver. 13.0.14 software (Genetyx, Tokyo, Japan).

2.4. Phylogenic analysis

The phylogenic relationships of the RuV strains were analyzed by drawing a neighbor-joining tree with a kimura-2-parameter model with 739 nucleotides (nt) of the E1 regions of 44 RuV strains using a CLUSTALW ver. 1.83 application (http://www.ddbj.nig.ac.jp/Welcome-j.html). These 739 nt correspond to the minimum acceptable window defined by the World Health Organization [15]. The reliability of the tree was estimated with 1000 iterations of bootstrapping. Another phylogenic tree was similarly constructed using the entire genome sequences of six RuV strains and the neighbor-joining method with a kimura-2-parameter model.

2.5. Growth kinetics analysis

Monolayers of RK-13 cells in 12-well plates were incubated with RuV strains at a MOI of 0.01 for 1 h. After the incubation, the cells were washed three times with phosphate-buffered saline and cultured in 1 ml of MEM containing 2% bovine serum at 35 °C or 39 °C. The culture medium was collected at 0, 1, 2, 3, and 5 days post-infection (p.i.). The virus titers were determined by plaque assays.

2.6. Plaque assay

Monolayers of RK13 cells in 6-well plates were incubated with 0.1 ml of samples that had been serially diluted by 10-fold for 1 h at room temperature. After the incubation, the cells were cultured in 3 ml of MEM containing 2% bovine serum, 0.5% agarose, and 40 μg/ml DEAE-dextran (0.5% agarose-MEM) at 35 °C for 7 days. After this culture period, 2 ml of 0.5% agarose-MEM containing 0.01% neutral red was overlaid on each well. The number of plaques were counted at 2 or 3 days after this procedure.

2.7. Plasmid construction

Plasmids encoding nonstructural protein (NSP)-derived peptides corresponding to amino acid positions 994–1548 ($NSP_{994-1548}$) [16] were constructed as follows. First-strand cDNAs were synthesized from purified viral RNA extracts from the TO-336.vac and KRT strains using SuperScript III reverse transcriptase (Invitrogen) and the 1548 reverse primer (5′-TATGAATTCGCCTACATGGATGCAGGC-3′) [16]. DNA fragments spanning nucleotide positions 994–1548 of the RuV genome were amplified by PCR using the 1548 reverse primer and the 994 forward primer (5′-AATGGATCCATGGACCACCGCCCGGCTGC-3′) [16]. The amplified DNA fragments were inserted into the mammalian cell expression plasmid pCMV-3tag-1a (Stratagene, Carlsbad, CA), in the downstream of a CMV promoter, using restriction enzyme recognition sites for *BamHI* and *EcoRI*, such that $NSP_{994-1548}$ was expressed as a peptide fused with three FLAG tags. Single point mutations were introduced into pCMV-3tag-1a encoding $NSP_{994-1548}$ using a KOD-plus- Mutagenesis Kit (Toyobo, Osaka, Japan).

2.8. Protein expression using plasmids and detection by immunoblotting

RK13 cells were transfected with pCMV-3tag-1a encoding $NSP_{994-1548}$ using the Lipofectamine LTX Plus reagent (Invitrogen) and cultured at 35 °C or 39 °C for 1 day or 3 days. In another experiment, transfected cells were cultured at 35 °C for 1 day, and subsequently, *de novo* protein synthesis was blocked by culturing the cells in medium containing 0.1 mg/ml cycloheximide at 35 °C or 39 °C for 2 days. After cell lysis, polypeptides were separated by electrophoresis in a polyacrylamide gel (10–20% gradient) in the presence of 0.1% sodium dodecyl sulfate and transferred onto nitrocellulose membranes. The membranes were incubated with anti-FLAG or anti-tubulin (clone B-5-1-2) antibodies (Sigma) followed by incubation with a peroxidase-conjugated secondary antibody. Peptides were then detected using an ECL Advance Western Blotting Detection Kit (GE Healthcare, Buckinghamshire, UK). The signal intensities were quantified using an LAS 1000plus Image Analyzer and the Image Gauge software (Fuji Film, Tokyo, Japan).

2.9. Detection of antibody titers in animals infected with RuV as a marker test

Specific pathogen-free female Hartley guinea pigs (weighing 300–400 g; 4, 8, or 12 animals per group) were infected subcutaneously with 5000 PFU of RuV. At 5 weeks p.i., the animals were euthanized and blood samples were obtained. The serum hemagglutination inhibition (HI) antibody titers were determined using goose erythrocytes and the hemagglutination antigen of RuV (Denka Seiken, Tokyo, Japan). Prior to the analyses, the serum specimens were treated with kaolin to remove nonspecific inhibitors and absorbed with goose erythrocytes to remove nonspecific hemagglutinins. After these treatments, the initial dilution of the samples was 1:8.

3. Results

3.1. TO-336.GMK5 and Matsuura.B3 strains are progenitors of or closely related to the progenitors of the currently used rubella vaccine strains

The growth kinetics of TO-336.GMK5, Matsuba.GMK3, and Matsuura.B3 were analyzed at 35 °C and 39 °C, and compared with those of the vaccine strains. The RVi/Hiroshima.JPN/01.03 wt strain was also evaluated as a control. After infection at 35 °C, all the tested viruses grew well and reached infectious titers that ranged from 10^4 to 10^6 PFU/ml at 5 days p.i. (Fig. 1A). At 39 C, TO-336.GMK5 and Matsuura.B3 grew productively and were similar to the RVi/Hiroshima.JPN/01.03 wt strain (Fig. 1B). In contrast, all of the vaccine strains showed abortive infections (Fig. 1B). Although Matsuba.GMK3 was able to replicate at 39 °C, its growth was severely restricted (Fig. 1B). These data show that TO-336.GMK5 and Matsuura.B3 have retained wt phenotypes with the capacity to grow at a high temperature, while Matsuba.GMK3 has a ts phenotype, although it is less severe than those of the vaccine strains.

Phylogenic analyses using 739 nt of the E1 regions (nucleotide positions 8731–9469) of 44 RuV strains revealed the relationships of the Matsuba.GMK3, TO-336.GMK5, and Matsuura.B3 strains with other RuV wt and vaccine strains (Fig. 2). The data suggested that TO-336.GMK5 was a direct progenitor strain of the currently used TO-336.vac strain. Similarly, the data indicated that Matsuura.B3 was closely related to a progenitor of the currently used Matsuura.vac strain (Fig. 2). On the other hand, Matsuba.GMK3 was apparently unrelated to the Matsuba.vac strain (Fig. 2).

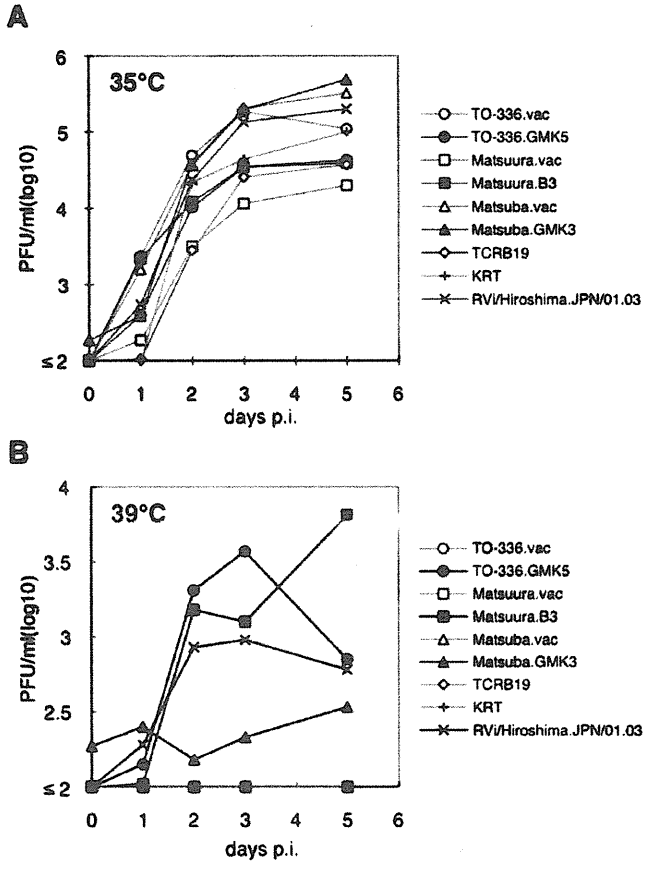

Fig. 1. Growth kinetics of RuV wt strains and vaccines at 35 °C and 39 °C. RK-13 cells were infected with RuV strains at a MOI of 0.01 and incubated at 35 °C (A) or 39 °C (B). The infectious titers of the culture supernatants were determined by plaque assays. Open circles, open squares, open triangles, open diamonds, and crosses indicate TO-336.vac, Matsuura.vac, Matsuba.vac, TCRB19, and KRT, respectively. Filled circles, filled squares, filled triangles, and saltires indicate TO-336.GMK5, Matsuura.B3, Matsuba.GMK3, and RVi/Hiroshima.JPN/01.03, respectively.

3.2. Japanese rubella vaccine strains have deletions in untranslated regions

The entire genome sequences of the TO-336.GMK5, Matsuba.GMK3, and Matsuura.B3 strains and three vaccine strains (Matsuba.vac, TCRB19, and Matsuura.vac) were determined. With the clarification of these sequences, the entire genome sequences became available for 13 RuV strains. These sequences included all five Japanese rubella vaccine (KRT [12], TO-336.vac [13], Matsuura.vac, TCRB19, Matsuba.vac), a US vaccine (RA27/3 [11]), and seven wt strains (Therien [10], M33 [11,14] (Gilliam S., GenBank X72393), TO-336wt [13], RVi/Matsue.JPN/68 [12], TO-336.GMK5, Matsuba.GMK3, and Matsuura.B3). Previous studies have indicated that the genome length of RuV is 9762 nt excluding the 5′ cap and 3′ poly(A) tract, and that the genome consists of a 40-nt 5′ untranslated region (UTR), a 6348-nt open reading frame (ORF) encoding two NSPs (P150 and P90), a 123-nt UTR, a 3189-nt ORF encoding three structural proteins (SPs) (C, E2, and E1), and a 62-nt 3′ UTR [11–13]. The genomes of Matsuba.GMK3, Matsuura.B3, and Matsuura.vac were also 9762 nt in length, and showed the same organization as the previously reported RuV strains [11–13]. On the other hand, the genome lengths of two Japanese vaccine

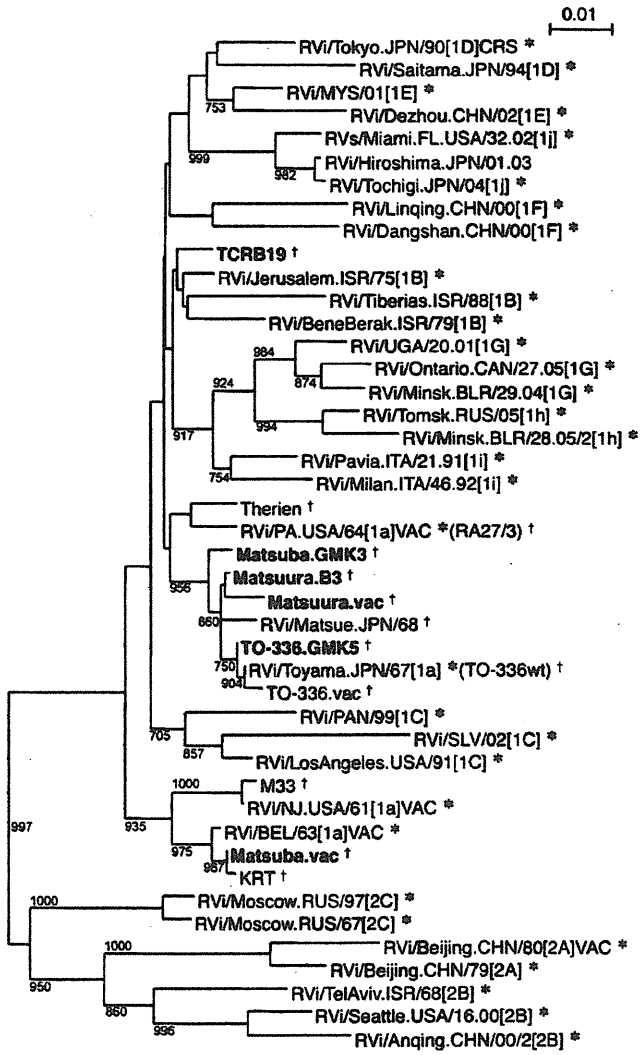

Fig. 2. Phylogenic tree of the 44 RuV strains. A phylogenic tree was drawn on the basis of 739 nt (positions 8731–9469) in the E1 regions of 44 RuV strains using a neighbor-joining method with a kimura-2-parameter model. Boldface characters indicate the strains whose entire genome sequences were determined in the present study. Asterisks indicate World Health Organization reference strains. Daggers indicate strains whose entire genome sequences are currently available. The genotypes based on the World Health Organization nomenclature are shown in square brackets. Bootstrap values above 700 (1000 replications) are shown on the phylogenic tree.

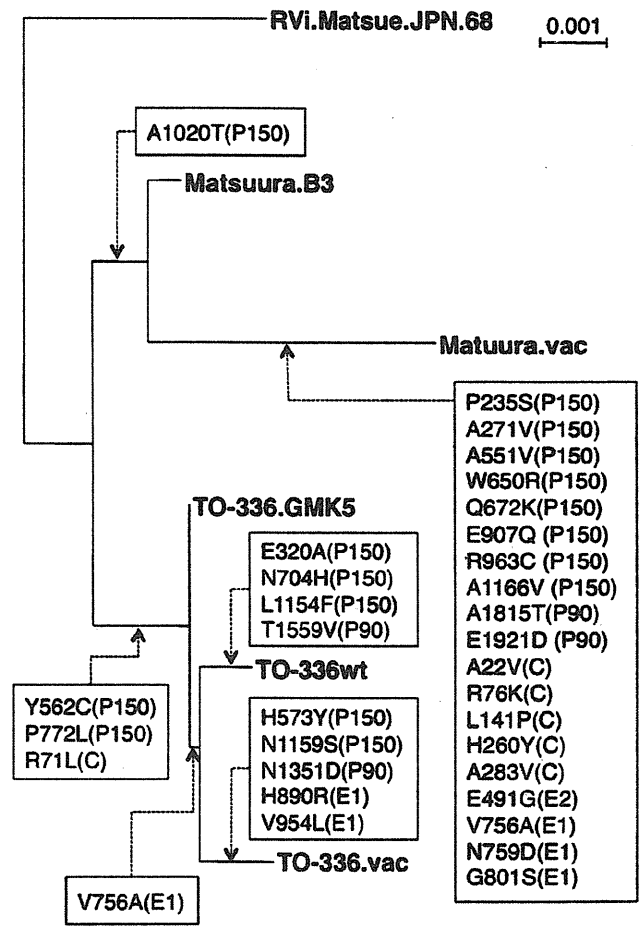

Fig. 3. Phylogenic relationships and amino acid substitutions in the Matsuura and TO-336 RuV strains. A phylogenic tree was drawn on the basis of the entire genome sequences of the Matsuura.B3, Matsuura.vac, TO-336.GMK3, TO-336 wt, TO-336.vac, and RVi/Matsue.JPN68 strains using a neighbor-joining method with a kimura-2-parameter model. The tree was rooted by the RVi/Matsue.JPN68 strain. Amino acid substitutions are indicated in boxes at the predicted points where they were introduced into the Matsuura and TO-336 strains.

strains, Matsuba.vac and TCRB19, were shorter by one nucleotide because of a single deletion in the UTR between the ORFs for the NSPs and SPs (junction UTR). The junction UTR is predicted to form secondary structures with a series of stem-loops [17] and to regulate subgenomic RNA synthesis [18]. Matsuba.vac and TCRB19 had a deletion (Δ) at nucleotide positions 6415 and 6479, respectively. Although neither position appeared to be directly involved in the stem-loop formation, this does not rule out the possibility that these deletions affect the functions of the junction UTR.

3.3. TO-336.vac has acquired six amino acid substitutions under the attenuation process

Kakizawa et al. [13] performed a sequence comparison analysis between TO-336.vac and a TO-336 wt strain (referred to as TO-336wt). They identified 10 amino acid differences between TO-336wt and TO-336.vac [13], while only six amino acid changes were found between TO-336.vac and TO-336.GMK5 (Figs. 3 and 4). A phylogenic tree drawn on the basis of the entire genome sequences revealed that TO-336.GMK5 was a progenitor of both TO-336.vac and TO-336wt (Fig. 4). The data suggested that TO-336wt was a descendant of TO-336.GMK5 with a different passage history from TO-336.vac (Fig. 3). These data are consistent with a previous report regarding the passage history of TO-336wt [19]. A comparison of the amino acid sequences and the phylogenic tree data suggested that TO-336.vac had acquired six substitutions, H573Y and N1159S in P150, N1351D in P90, and V756A, H890R, and V954L in E1, during the passage history of the virus (Fig. 3). N1159S and N1351D were located in the protease domain of P150 and the helicase domain of P90, respectively [20–23] (Fig. 4). Zhou et al. [24] recently reported that a 32-mer peptide region (amino acid positions 1152–1183) within the protease domain acts as a calmodulin-binding domain (CaMBD) that mainly adopts a helical structure and plays crucial roles in the protease activity and virus infectivity. N1159S was located in this helical structure. The V756A substitution in E1 was also found in TO-336wt (Figs. 3 and 4B), and was therefore not reported by Kakizawa et al. [13]. TO-336wt possessed four additional substitutions (E320A, N704H, and L1154F in P150 and T1559V in P90) (Fig. 3). These mutations were unique to TO-336wt

(Fig. 4). Kakizawa et al. [13] reported that TO-336.vac also possesses a unique residue (arginine) at position 501 of P150. However, this residue was not found in our analyses. The TO-336.vac strain used in the present study possessed the same residue as TO-336.GMK5 and TO-336wt at that position.

3.4. Matsuura.vac has acquired 19 amino acid substitutions under the attenuation process

From the nucleotide sequence data, 19 amino acid differences were predicted between Matsuura.B3 and Matsuura.vac

A

		MT																					
		3	42	235	271	289	295	320	323	362	407	427	433	466	473	483	491	503	514	529	541	551	555	562
Wt	M33	K	T	P	A	V	T	E	W	S	S	D	F	L	K	T	A	V	P	R	A	A	L	Y
	Matsuba.GMK5	K	T	P	A	L	T	E	R	S	S	D	F	L	K	T	A	V	P	R	A	A	L	Y
	Matsue.JPN68	K	T	P	A	V	T	E	R	S	G	D	F	F	K	T	A	A	P	R	A	A	L	Y
	TO-336wt	K	T	P	A	V	T	A	R	S	S	D	F	L	K	T	A	A	P	R	A	A	L	C
	TO-336.GMK5	K	T	P	A	V	T	E	R	S	S	D	F	L	K	T	A	A	P	R	A	A	L	C
	Matsuura.B3	K	T	P	A	V	T	E	R	S	S	D	F	L	K	T	A	A	P	R	A	A	L	Y
	Therien	K	T	P	A	V	T	E	R	C	G	D	L	L	K	T	E	V	Q	R	A	A	P	Y
Vac	Matsuba.vac	K	T	P	A	V	A	E	R	S	S	D	F	L	K	T	A	A	P	R	A	A	L	Y
	KRT	K	T	P	A	V	A	E	R	S	S	D	F	L	K	A	A	A	P	R	A	A	L	Y
	TO-336.vac	K	T	P	A	V	T	E	R	S	S	D	F	L	K	T	A	A	P	R	A	A	L	C
	Matsuura.vac	K	T	S	V	V	T	E	R	S	S	D	F	L	K	T	A	A	P	R	A	V	L	Y
	TCRB19	K	T	P	A	V	T	E	R	S	S	D	F	L	Q	T	A	V	P	R	A	A	L	Y
	RA27/3	R	S	P	A	V	T	E	R	S	S	G	F	L	K	T	A	V	P	H	V	A	L	Y

		573	584	604	606	650	672	674	697	699	702	704	715	717	720	722	732	739	740	751	756	758	767	772
Wt	M33	H	G	R	Y	W	K	I	R	T	E	N	G	L	T	P	R	H	S	V	R	Q	V	P
	Matsuba.GMK5	H	E	R	F	W	Q	I	G	A	D	N	G	S	T	S	R	H	L	A	P	A	A	P
	Matsue.JPN68	H	E	R	F	W	Q	I	G	A	D	N	G	S	T	P	R	H	L	A	P	A	A	P
	TO-336wt	H	E	R	F	W	Q	I	G	A	D	H	G	S	T	P	R	H	L	A	P	A	A	L
	TO-336.GMK5	H	E	R	F	W	Q	I	G	A	D	N	G	S	T	P	R	H	L	A	P	A	A	L
	Matsuura.B3	H	E	R	F	W	Q	I	G	A	D	N	G	S	T	P	R	H	L	A	P	A	A	P
	Therien	H	E	R	F	W	Q	I	G	A	D	N	R	S	A	P	R	H	S	A	P	A	A	P
Vac	Matsuba.vac	H	E	R	F	W	Q	V	G	A	D	N	G	L	T	P	R	P	S	V	P	A	A	P
	KRT	H	E	R	F	W	Q	V	G	A	D	N	G	L	T	P	R	P	S	V	P	A	A	P
	TO-336.vac	Y	E	R	F	W	Q	I	G	A	D	N	G	S	T	P	R	H	L	A	P	A	A	L
	Matsuura.vac	H	E	R	F	R	K	I	G	A	D	N	G	S	T	P	R	H	L	A	P	A	A	P
	TCRB19	H	E	C	F	R	Q	I	G	A	D	N	G	P	T	P	R	H	S	A	P	A	A	P
	RA27/3	H	E	R	F	W	Q	I	G	A	D	N	G	S	T	S	C	H	S	A	P	A	A	P

											X								Pro					
		774	775	777	784	790	791	795	799	801	865	874	900	907	930	958	961	963	1002	1007	1020	1042	1115	1117
Wt	M33	T	T	E	H	V	Y	G	S	K	D	I	R	E	R	A	A	R	S	D	A	Y	Q	M
	Matsuba.GMK5	T	S	G	H	A	Y	D	P	K	D	T	Q	E	C	A	A	R	T	D	A	Y	Q	M
	Matsue.JPN68	T	S	G	H	A	Y	D	S	K	D	T	R	E	C	A	A	R	S	D	A	Y	Q	M
	TO-336wt	T	S	G	H	A	Y	D	P	K	D	T	R	E	C	A	A	R	S	D	A	Y	Q	M
	TO-336.GMK5	T	S	G	H	A	Y	D	P	K	D	T	R	E	C	A	A	R	S	D	A	Y	Q	M
	Matsuura.B3	T	S	G	H	A	Y	D	P	K	D	T	R	E	C	A	A	R	S	D	T	Y	Q	M
	Therien	I	P	G	D	A	C	G	S	R	N	T	R	E	C	T	V	R	S	D	A	Y	H	M
Vac	Matsuba.vac	T	S	E	H	V	Y	G	S	K	D	T	R	E	C	A	V	R	S	G	A	H	Q	M
	KRT	T	S	E	H	V	Y	G	S	K	D	T	R	E	C	A	V	R	S	G	A	H	Q	M
	TO-336.vac	T	S	G	H	A	Y	D	P	K	D	T	R	E	C	A	A	R	S	D	A	Y	Q	M
	Matsuura.vac	T	S	G	H	A	Y	D	P	K	D	T	R	Q	C	A	A	C	S	D	T	Y	Q	M
	TCRB19	T	S	G	D	A	Y	G	S	K	D	T	R	E	C	T	A	R	S	D	A	C	Q	M
	RA27/3	T	S	G	D	A	Y	G	S	K	D	T	R	E	R	T	A	R	S	D	A	Y	Q	V

		Pro									Hel									RdRp		
		1140	1154	1159	1166	1177	1190	1191	1199	1209	1337	1351	1393	1403	1466	1497	1559	1583	1639	1767	1815	1921	1979
Wt	M33	V	L	N	A	K	H	E	W	P	I	N	D	A	G	T	T	L	R	T	A	E	N
	Matsuba.GMK5	V	L	N	A	K	H	E	R	P	V	N	D	A	E	T	T	S	R	A	A	E	S
	Matsue.JPN68	V	L	N	A	K	H	E	R	P	V	N	D	A	E	T	T	S	R	A	A	E	S
	TO-336wt	V	F	N	A	K	H	E	R	P	V	N	D	A	E	T	V	S	R	A	A	E	S
	TO-336.GMK5	V	L	N	A	K	H	E	R	P	V	N	D	A	E	T	T	S	R	A	A	E	S
	Matsuura.B3	V	L	N	A	K	H	E	R	P	V	N	D	A	E	T	T	S	R	A	A	E	S
	Therien	A	L	N	A	K	H	E	R	P	V	N	D	R	E	T	T	S	R	A	A	E	S
Vac	Matsuba.vac	V	L	N	A	K	H	E	R	P	V	N	D	A	E	I	T	S	C	A	A	E	S
	KRT	V	L	N	A	K	H	E	R	P	V	N	D	A	E	I	T	S	R	A	A	E	S
	TO-336.vac	V	L	S	A	K	H	E	R	P	V	D	D	A	E	T	T	S	R	A	A	E	S
	Matsuura.vac	V	L	N	V	K	H	E	R	P	V	N	D	A	E	T	T	S	R	A	T	D	S
	TCRB19	V	L	N	A	K	R	E	R	P	V	N	D	A	E	T	T	S	R	A	A	E	S
	RA27/3	V	L	N	A	R	H	K	R	S	V	N	E	A	E	T	T	S	R	A	A	E	S

Fig. 4. Comparison of the amino acid residues among seven RuV wt strains and six vaccines. The amino acid sequences were compared among 13 RuV strains (seven wt strains and six vaccines), and residues with variations were noted. (A) NSPs. (B) SPs. Shaded symbols indicate amino acid residues in minority groups among the 13 strains. Numbers indicate the amino acid positions. Known or predicted functional domains [20,22,44,45] are indicated in the top rows. MT: methyltransferase domain; X: X domain; Pro: protease domain; Hel: helicase domain; RdRp: RNA-dependent RNA polymerase domain; C_{SP}: signal peptide of the capside protein; $E2_{TM}$: transmembrane domain of E2; $E1_{TM}$: transmembrane domain of E1.

B

C

		11	18	22	26	34	48	60	64	67	69	71	72	76	87	95	141	175	226	254	260	283
Wt	M33	D	A	A	G	S	T	P	R	A	A	R	K	R	S	K	L	I	T	T	H	A
	Matsuba.GMK5	D	A	A	E	S	S	R	G	G	G	R	R	R	S	K	L	T	T	S	H	V
	Matsue.JPN68	A	A	A	E	S	S	R	G	G	G	R	R	R	S	K	L	T	T	S	H	A
	TO-336wt	D	A	A	E	S	S	R	G	G	G	L	R	R	S	K	L	T	T	S	H	A
	TO336.GMK5	D	A	A	E	S	S	R	G	G	G	L	R	R	S	K	L	T	T	S	H	A
	Matsuura.B3	D	A	A	E	S	S	R	G	G	G	R	R	R	S	K	L	T	T	S	H	A
	Therien	D	A	A	E	S	S	R	G	G	G	R	R	R	T	K	L	T	T	S	H	A
Vac	Matsuba.vac	G	A	A	E	P	S	R	G	G	G	R	K	R	S	K	L	T	T	S	H	A
	KRT	G	A	A	E	P	S	R	G	G	G	R	K	R	S	K	L	T	S	S	H	A
	TO-336.vac	D	A	A	E	S	S	R	G	G	G	L	R	R	S	K	L	T	T	S	H	A
	Matsuura.vac	D	A	V	E	S	S	R	G	G	G	R	R	K	S	K	P	T	T	S	Y	V
	TCRB19	D	A	A	E	S	S	R	G	G	G	R	R	R	S	E	L	T	T	S	H	A
	RA27/3	D	T	A	E	S	T	R	G	G	G	R	R	R	T	K	L	T	T	S	H	A

		C_{TP}	E2																$E2_{TM}$		E2	$E2_{TM}$
		292	306	307	313	314	319	351	404	405	411	412	413	422	446	485	491	505	534	535	539	558
Wt	M33	A	A	D	M	P	R	H	S	L	Y	I	A	P	Y	I	E	T	S	L	F	A
	Matsuba.GMK5	A	A	D	T	L	R	H	P	L	S	T	T	A	H	V	E	T	S	L	V	A
	Matsue.JPN68	A	A	D	T	L	R	H	P	F	S	T	T	A	H	V	E	T	S	L	L	A
	TO-336wt	A	A	D	T	L	R	H	P	F	S	T	T	A	H	V	E	T	S	L	L	A
	TO336.GMK5	A	A	D	T	L	R	H	P	F	S	T	T	A	H	V	E	T	S	L	L	A
	Matsuura.B3	A	A	D	T	L	R	H	P	F	S	T	T	A	H	V	E	T	S	L	L	A
	Therien	T	A	D	T	L	C	Y	P	L	S	T	T	A	H	V	E	A	S	L	L	A
Vac	Matsuba.vac	A	V	H	T	P	R	H	S	L	S	T	T	P	H	V	E	T	P	P	L	A
	KRT	A	V	H	T	P	R	H	S	L	S	T	T	P	H	V	E	T	P	P	L	A
	TO-336.vac	A	A	D	T	L	R	H	P	F	S	T	T	A	H	V	E	T	S	L	L	A
	Matsuura.vac	A	A	D	T	L	R	H	P	F	S	T	T	A	H	V	Q	T	S	L	L	A
	TCRB19	A	A	D	T	L	R	H	P	L	S	T	T	A	H	V	E	T	S	L	L	A
	RA27/3	A	A	D	T	L	R	H	P	L	S	T	T	A	H	V	E	T	S	L	L	T

		E1																			$E1_{TM}$
		587	599	609	650	756	759	785	792	801	873	890	915	919	953	954	959	962	980	991	1041
Wt	M33	T	T	G	T	V	N	L	Y	G	I	H	A	A	T	V	V	F	Q	T	P
	Matsuba.GMK5	T	T	R	T	V	N	L	Y	G	I	H	A	A	T	V	V	F	Q	S	L
	Matsue.JPN68	T	T	R	T	V	N	L	Y	G	I	H	A	A	T	V	V	F	Q	S	L
	TO-336wt	T	T	R	T	A	N	L	Y	G	I	H	A	A	T	V	V	F	Q	S	L
	TO336.GMK5	T	T	R	T	V	N	L	Y	G	I	H	A	A	T	V	V	F	Q	S	L
	Matsuura.B3	T	T	R	T	V	N	L	Y	G	I	H	A	A	T	V	V	F	Q	S	L
	Therien	T	A	R	A	V	N	L	Y	G	I	H	A	T	T	V	L	V	Q	T	P
Vac	Matsuba.vac	A	T	R	T	V	D	M	Y	G	I	H	T	A	T	V	V	F	Q	S	L
	KRT	A	T	R	T	V	D	M	Y	G	I	H	T	A	T	V	V	F	R	S	L
	TO-336.vac	T	T	R	T	A	N	L	Y	G	I	R	A	A	T	L	V	F	Q	S	L
	Matsuura.vac	T	T	R	T	A	D	L	Y	S	I	H	A	A	T	V	V	F	Q	S	L
	TCRB19	T	A	R	T	V	N	L	Y	G	M	H	A	A	A	V	V	F	Q	S	L
	RA27/3	T	A	R	T	V	N	L	H	G	I	H	A	T	T	L	L	F	Q	S	L

Fig. 4. (Continued).

(Figs. 3 and 4). Except for the A1020T substitution in P150, Matsuura.B3 possessed the identical amino acid sequence to the consensus sequence among the other three wt strains, TO-336.GMK5, RVi/Matsue.JPN/68, and Matsuba.GMK3, in the same cluster (Figs. 2 and 4). These data suggest that Matsuura.vac acquired the 19 amino acid substitutions under the attenuation process (Fig. 3). Eight of these substitutions were in P150 (Figs. 3 and 4). Among these substitutions, P235S was in the methyltransferase (MT) domain [20,22], E907Q and R963C were in the X domain with unknown functions [20,21], and A1166V was in the protease domain [20–23] (Fig. 4A). A1166V was also located in the helical structure of the CaMBD (amino acid positions 1152–1183) in the protease domain [24]. Two substitutions (A1815T and E1921D) were found in P90, and both were located in the RNA-dependent RNA polymerase domain [20,21] (Fig. 4A). The C, E2, and E1 SPs had five, one, and three substitutions, respectively (Fig. 4B).

3.5. No common substitutions are found in vaccine strains, but some substitutions are shared by specific vaccine strains

Matsuba.vac and KRT shared many amino acid substitutions (Fig. 4). TCRB19 and RA27/3 also shared some amino acid substitutions (Fig. 4). However, despite these common features of the Japanese rubella vaccine strains, no consensus amino acid changes were found among them (Fig. 4). Regarding the molecular determinant for the ts phenotype, Sakata et al. [12] suggested that a Y1042H substitution in P150 is responsible for the ts phenotype of KRT. Matsuba.vac possessed the same substitution (Fig. 4A). Interestingly, TCRB19 also had a tyrosine-to-cysteine substitution at the same position (Fig. 4A). Therefore, KRT, Matuba.vac, and TCRB19 may exhibit the ts phenotype via the same molecular mechanism.

3.6. TO-336.vac has acquired wt phenotypes by second-site mutations in the protease domain of P150

A TO-336.vac-derived mutant clone, designated TO-336.rev, was generated by passages of TO-336.vac in RK13 cells at 39 °C. Unlike TO-336.vac, TO-336.rev was able to replicate in RK13 cells at 39 °C, and its virus titer at 5 days p.i. was as high as that of TO-336.GMK5 (Fig. 5). The entire genome sequence of TO-336.rev was determined, and compared with that of TO-336.vac. A total of nine nucleotide substitutions were found in the genome of TO-336.rev (Table 1). Two of these substitutions were non-synonymous, and both were located in the protease domain of P150 (Table 1). These mutations caused asparagine-to-threonine and alanine-to-valine substitutions at amino acid positions 1126 and 1277 (N1126T

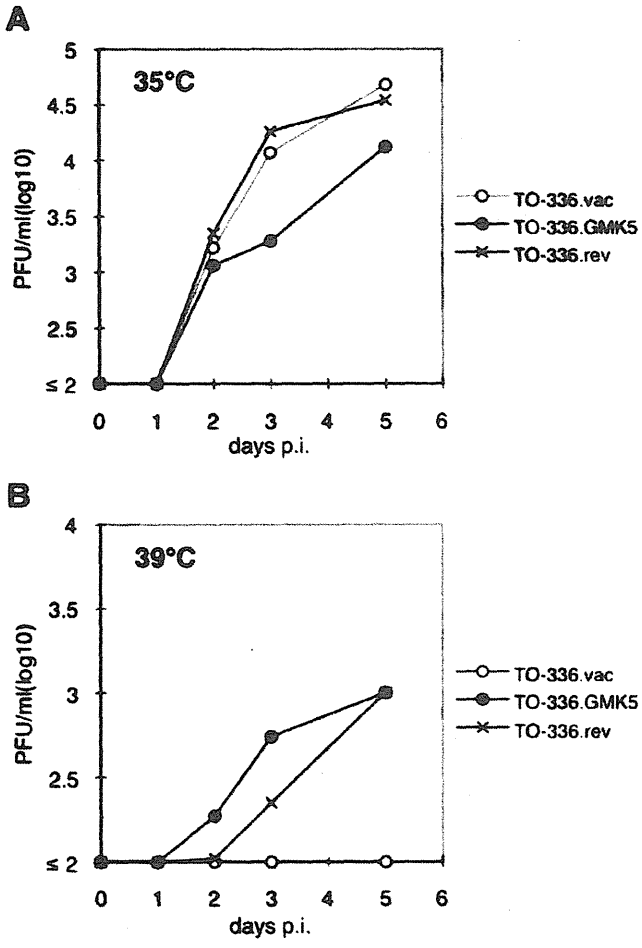

Fig. 5. Growth kinetics of TO-336.rev at 35 °C and 39 °C. RK-13 cells were infected with RuV strains at a MOI of 0.01 and incubated at 35 °C (A) or 39 °C (B). The infectious titers of the culture supernatants were determined by plaque assays. Closed and open circles indicate TO-336.GMK5 and TO-336.vac, respectively. Saltires indicate TO-336.rev.

and A1277V), respectively (Table 1). TO-336.vac possessed three amino acid substitutions in the NSPs compared with TO-336.GMK5 (Figs. 3 and 4A). Therefore, N1126T and A1277V were not direct reversions to the residues of TO-336.GMK5, but instead were second-site mutations that rendered TO-336.vac able to grow at 39 °C. These data brought the protease domain of the P150 protein to our attention.

3.7. Reduced stability of an NSP-derived peptide at 39 °C is correlated with reduced virus growth at that temperature (ts phenotype)

Chen et al. [16] analyzed the protease activities of RuV NSPs using NSP-derived peptides of varying lengths. We used one of these NSP-derived peptides corresponding to amino acid positions 994–1548 possessing FLAG tags at the amino-terminus ($NSP_{994-1548}$). Since the peptide retains the ability to cleave itself behind the amino acid position 1301 [16], the anti-FLAG antibody was expected to detect both uncleaved and cleaved forms of the peptide. The $NSP_{994-1548}$ peptide of TO-336.vac (TO-336.vac-$NSP_{994-1548}$) and that containing the residues of TO-336.GMK5 at positions 1159 and 1351 (TO-336.vac-$NSP_{994-1548}$(S1159N/D1351N)) were expressed in cells at 35 °C or 39 °C (Fig. 6A, TO-336.vac and S1159N/D1351N). A TO-336.vac-$NSP_{994-1548}$ mutant (C1152S), which lacks the protease activity, was expressed as a control (Fig. 6A, C1152S). Both the TO-336.vac-$NSP_{994-1548}$ and TO-336.vac-$NSP_{994-1548}$(S1159N/D1351N) were cleaved efficiently, and much stronger signals were detected for cleaved forms, when compared to the signals for uncleaved forms, at both temperatures (Fig. 6A). These data showed that the protease activity of TO-336.vac is not significantly affected by the mutations at positions 1159 and 1351. However, it was noted that the expression level of TO-336.vac-$NSP_{994-1548}$ became lower than those of TO-336.vac-$NSP_{994-1548}$(S1159N/D1351N) at 39 °C (Fig. 6A). It was more evident, when expression levels were analyzed at 3 days posttransfection (Fig. 6B) than at 1 day posttransfection (Fig. 6A). TO-336.vac-$NSP_{994-1548}$ peptides with the residues of TO-336.rev at positions 1126 and/or 1277 also showed similar protease activities (Fig. 6C). These peptides with various mutations were expressed in cells at 35 °C, and subsequently cultured

Table 1
Nucleotide and amino acid differences between TO-336.vac and the related viruses.

Region	Nucleotide				Amino acid			
	Position	TO-336.GMK5	TO-336.vac	TO-336.rev	Position	TO-336.GMK5	TO-336.vac	TO-336.rev
5′ UTR	36	U	C	C	N/A			
P	448	U	C	C	136	–	–	–
150	1327	U	C	C	429	–	–	–
	1708	U	C	C	556	–	–	–
	1757	C	U	U	573	His	Tyr	Tyr
	3417	A	A	C	1126	Asn	Asn	Thr
	3516	A	G	G	1159	Asn	Ser	Ser
	3781	C	C	U	1247	–	–	–
	3793	C	C	A	1251	–	–	–
	3870	C	C	U	1277	Ala	Ala	Val
	3946	U	U	C	1302	–	–	–
P90	4091	A	G	G	1351	Asn	Asp	Asp
J-UTR	6463	C	C	A	N/A			
C	6583	C	U	U	24	–	–	–
	6649	C	U	U	46	–	–	–
	6958	C	U	U	149	–	–	–
E1	8778	U	C	C	756	Val	Ala	Ala
	9013	U	U	C	834	–	–	–
	9180	A	G	G	890	His	Arg	Arg
	9371	G	C	C	954	Val	Leu	Leu
3′	9712	U	U	C	N/A			
UTR	9742	C	C	U	N/A			

N/A: not applicable, –: silent mutation.

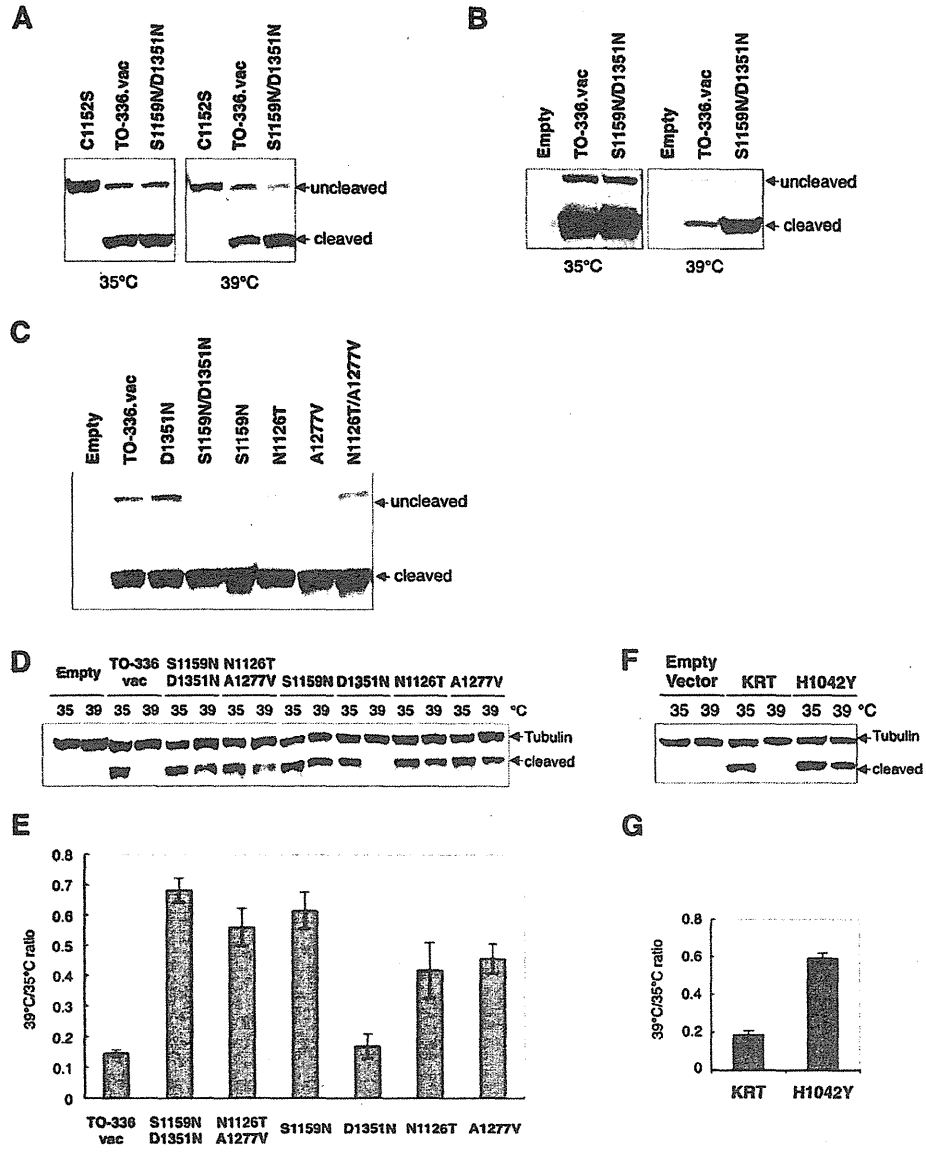

Fig. 6. Analysis of the thermal stabilities of NSP-derived peptides. (A and B) Using expression plasmids, an $NSP_{994-1548}$ peptide of TO-336.vac (TO-336.vac-$NSP_{994-1548}$) and that possessing the amino acid substitutions S1159N and D1351N (TO-336.vac-$NSP_{994-1548}$(S1159N/D1351N)) were expressed in cells at 35 °C or 39 °C. TO-336.vac-$NSP_{994-1548}$ possessing a C1152S mutation was also expressed as a control to show an uncleaved form of the peptide. Expression levels were analyzed at 1 day (A) and 3 days (B) after transfection of the plasmids. Empty; an expression plasmid lacking an $NSP_{994-1548}$ insert. (C) TO-336.vac-$NSP_{994-1548}$ peptides possessing the amino acid substitutions S1159N, D1351N, D1126T, and A1277V individually or in combination were expressed in cells at 35 °C, and expression levels were analyzed at 1 day after transfection of the plasmids. Empty; an expression plasmid lacking an $NSP_{994-1548}$ insert. (D) An $NSP_{994-1548}$ peptide of TO-336.vac (TO-336.vac-$NSP_{994-1548}$) and those possessing the amino acid substitutions S1159N, D1351N, D1126T, and A1277V individually or in combination was expressed in cells at 35 °C using expression plasmids. After 1 day of culture with the expression plasmids at 35 °C, the cells were cultured with cycloheximide to inhibit *de novo* protein synthesis for 2 days at 35 °C or 39 °C. Tubulin was detected as an internal control. Empty; an expression plasmid lacking an $NSP_{994-1548}$ insert. (E) Quantification of the data shown in (D). The ratios of the expression levels of the NSP peptides(cleaved form) at 39 °C and 35 °C are shown. The data represent the means ± standard errors of triplicate experiments. (F) $NSP_{994-1548}$ of KRT (KRT-$NSP_{994-1548}$) and that possessing an H1042Y substitution (KRT-$NSP_{994-1548}$(H1024Y)) were subjected to the same experiments described for (D). (G) Quantification of the data shown in (F). The data represent the means ± standard errors of triplicate experiments.

with cycloheximide to inhibit *de novo* synthesis of the peptides for 2 days at 35 °C or 39 °C (Fig. 6D). Fig. 6E shows the ratios of expression levels of the peptide ($NSP_{994-1301}$) at 39 °C and 35 °C (39 °C/35 °C ratios). Only cleaved forms, $NSP_{994-11301}$, were shown, since uncleaved forms were barely detectable. These data showed that TO-336.vac-$NSP_{994-1301}$ was unstable at 39 °C (Figs. 6D and E, TO-336.vac), whereas TO-336.vac-$NSP_{994-1301}$(S1159N/D1351N) was stable (Figs. 6D and 7E, S1159N/D1351N). A peptide containing the residues of TO-336.rev at positions 1126 and 1277 (TO-336.vac-$NSP_{994-1301}$(N1126T/A1277V)) also exhibited high stability at 39 °C (Figs. 6D and E, N1126T/A1277V). The effects of individual mutations at positions 1159, 1351, 1126, and 1277 were analyzed. The data revealed that the peptide possessing S1159N was as stable as TO-336.vac-$NSP_{994-1301}$(S1159N/D1351N) (Figs. 6D and E, S1159N). The D1351N substitution had no effect on the stability of $NSP_{994-1301}$ at 39 °C (Figs. 6D and E, D1351N). These data suggest that the N1159S mutation causes the ts phenotype of TO-336.vac, and that N1351D only exerts a neutral effect. On the other hand, both types of peptides with N1126T or A1277V showed moderate stability at 39 °C (Figs. 6D and E, N1126T and A1277V). These data

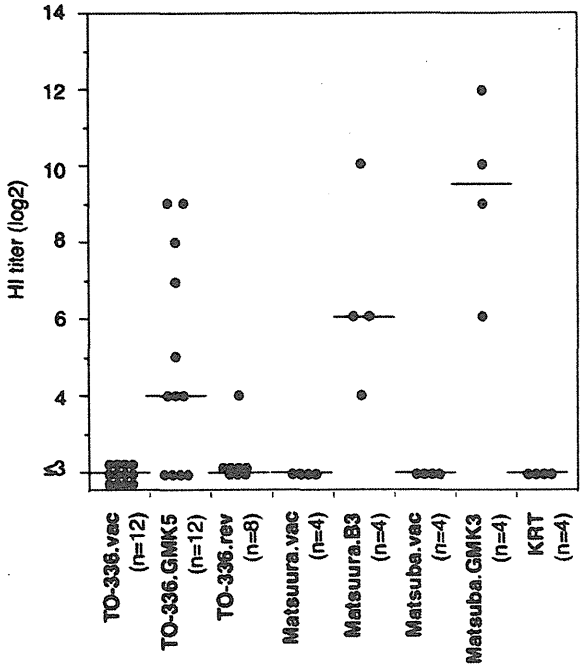

Fig. 7. Production of HI antibodies in guinea pigs inoculated with RuV strains. Guinea pigs (4, 8, or 12 animals per RuV strain) were subcutaneously inoculated with 5000 PFU of RuV. The serum HI antibody titers were measured at 5 weeks p.i. The horizontal bars indicate the median values of the HI antibody titers of the animals inoculated with each RuV strain.

suggest that both of the mutations contribute to the phenotypic reversion of TO-336.rev.

The Y1042H substitution in P150 is known to be responsible for the ts phenotype of KRT [12]. The $NSP_{994-1548}$ peptide of KRT (KRT-$NSP_{994-1548}$) was also subjected to the expression analysis. A strong signal for KRT-$NSP_{994-1301}$ was detected in cells incubated at 35 °C, while only a faint signal was detected in cells incubated at 39 °C (Figs. 6F and G, KRT). A histidine residue at amino acid position 1042 of NSP was replaced with tyrosine, the wt residue. This mutation (H1042Y) made the KRT-$NSP_{994-1301}$ stable at 39 °C (Figs. 7F and G, H1042Y). Therefore, the amino acid residues at 1042, 1126, 1159, and 1277, which are located in the protease domain, seem to be individually involved in the thermal stability of $NSP_{994-1301}$.

Collectively, the data suggest that substitutions in the protease domain may be predisposed to cause thermal lability of the NSPs, conferring the ts phenotype on some rubella vaccine strains.

3.8. A high growth capacity of RuV in cultured cells at a high temperature is neither essential nor sufficient to elicit antibody responses in guinea pigs

Japanese rubella vaccines lack the ability to elicit anti-RuV antibodies in experimentally infected guinea pigs and rabbits [6]. This is used as an *in vivo* marker phenotype of Japanese rubella vaccine strains [6]. According to the protocol for a marker test of rubella vaccines documented in the MRBP [8,9], 5000 PFU of each wt or vaccine strain was inoculated subcutaneously into guinea pigs, and their HI antibody titers were analyzed at 5 weeks after the inoculation. HI antibody titers were undetectable in the sera of all animals inoculated with vaccine strains (TO-336.vac, Matsuura.vac, Matsuba.vac, and KRT) (Fig. 7). The TO-336.GMK5 and Matsuura.B3 strains induced anti-RuV antibody responses in 66.7% and 100% of the inoculated animals, respectively (Fig. 7). It was noteworthy that all of the animals inoculated with Matsuba.GMK3, which showed a moderate ts phenotype (Fig. 1B), produced high HI titers (Fig. 7). The median value of the HI titers induced by Matsuba.GMK3 was even higher than those induced by TO-336.GMK5 and Matsuura.B3 (Fig. 7). The reversion mutant, TO-336.rev, which was able to replicate at a high temperature (Fig. 5B), hardly induced any antibody responses in the animals (Fig. 7). Most of the animals were seronegative, and only one of eight animals showed a low HI titer (Fig. 7). These findings demonstrate that the ability of RuV to grow at a high temperature was not necessarily correlated with the potency to elicit humoral immune responses in guinea pigs.

4. Discussion

Many vaccine strains for live attenuated vaccines have been successfully generated by adaptation of clinical isolates through numerous passages in various cultured cells [6,25–28]. During this process, the viruses have often been propagated at low temperatures (29–35 °C), and have acquired the ts phenotype [6,26,28]. Although these adaptations often reduce viral virulence, the molecular mechanisms of the attenuation have been poorly elucidated. Comparisons of nucleotide and amino acid sequences between vaccine strains and their progenitors provide basic and solid information toward understanding of the molecular bases that underlie the attenuation and the acquisition of other unique phenotypes of vaccine strains. In the present study, we determined the entire nucleotide sequences of the progenitors of currently used rubella vaccine strains. Unfortunately, the detailed records of the old isolates were unavailable. The passage histories of two viruses, however, could be predicted from their strain names, since the names of vaccine progenitors are usually designated on the basis of their passage history [6]. TO-336.GMK5 and Matsuba.GMK3 seemed to have been isolated in GMK cells and passaged in these cells five and three times, respectively. However, the history of Matsuura.B3 was unclear. In addition to these viruses, the entire genome nucleotide sequences of three Japanese rubella vaccines (Matsuba.vac, TCRB19, and Matsuura.vac) were determined. Phylogenic analyses confirmed that TO-336.GMK5 and Matsuura.B3 were progenitors or closely related progenitors of the currently used TO-336.vac and Matsuura.vac strains, respectively, whereas Matsuba.GMK3 was apparently unrelated to the currently used Matsuba.vac strain. However, it could be the progenitor of a vaccine candidate that has not been licensed. Comparative analyses of these strains and other RuV strains provided full lists of the mutations introduced into the genomes of TO-336.vac and Matsuura.vac during their passages under laboratory conditions. Matsuura.vac had acquired greater number of amino acid substitutions than TO-336.vac. This may be caused by differences in the host cell types used to produce these vaccine strains and/or the numbers of passages in these cells. TO-336.vac was generated after seven passages in GMK cells, followed by 20 passages in guinea pig kidney cells and three passages in rabbit kidney cells at 29–32 °C [6,19]. Matsuura.vac was generated after 14 passages in GMK cells, 65 passages in chick embryo amniotic cavities, and 11 passages in Japanese quail embryo fibroblasts at 32–35 °C [6,19].

A single amino acid substitution, Y1042H, has been demonstrated to be responsible for the ts phenotype of the KRT vaccine strain [12]. This mutation is located in the protease domain of P150 [20]. TO-336.vac became able to grow at a high temperature by acquiring second-site mutations in the protease domain. Therefore, we focused on the mutations in the protease domain for determining the ts phenotype. The protease domain possesses a cysteine-rich Ca^{2+} and Zn^{2+}-binding domain, which is essential for the protease activity and virus replication [29,30]. This domain contains a CaMBD with an alpha-helical structure, which also plays important roles in the protease activity and virus

replication [24]. Mutations in this domain have been shown to reduce its conformational stability at a high temperature [29]. The ts phenotype-determining mutation, Y1042H, found in the KRT vaccine strain rendered the protease domain-containing peptide, $NSP_{994-1301}$, unstable at a high temperature. In contrast, the N1126T and A1277V mutations found in the reversion mutant, TO-336.rev, rendered the TO-336.vac-derived $NSP_{994-1301}$ thermostable. Thus, the present data suggest that reduced stability of the conformation of the protease domain of P150 at a high temperature is a cause of the ts phenotype of some rubella vaccine strains. RuV with any mutations that have similar effects on the protease domain may exhibit a ts phenotype. It is of interest that other vaccine strains also possessed unique mutations in the protease domain.

The most important properties of vaccines are their safety and efficacy. For attenuated live vaccines, avirulence is critical for safety. Therefore, understanding of the molecular bases of the attenuation is crucial for quality control of vaccines. However, no reliable animal models for analyzing RuV virulence have been established. Humans are the only natural host for RuV, and it exhibits poor infection and replication in experimentally infected animals. Nonetheless, infections with clinical isolates of RuV induce considerable levels of humoral immune responses in animals, and the lack of these responses in the majority (>80%) of infected guinea pigs has been used as an *in vivo* marker of licensed rubella vaccines in Japan [6]. This phenotype is documented in the MRBP [8,9]. Although the low potency to induce antibody responses may be correlated with the attenuated phenotype of vaccine strains, no scientific evidence has been provided. A marker test that checks the *in vivo* marker phenotype of vaccine strains has been performed to verify the constancy of the vaccine quality, but not the avirulence [8,9]. It is difficult to determine the safety or avirulence of vaccines using cell culture systems. However, it is generally accepted that a ts phenotype, which can be analyzed in cultured cells, may play a role in virus attenuation [31–37]. Mutations in various genes can cause the ts phenotypes of viruses [33–35,38–43]. Since the body temperatures of guinea pigs and rabbits range from 37.5 to 39.5 °C, the inability of rubella vaccine viruses to elicit humoral immune responses in these animals may be partly and reasonably explained by the ts phenotype [5]. Surprisingly, however, Matsuba.GMK3 with a partial ts phenotype was highly potent in eliciting humoral immune responses in animals. On the other hand, the reversion mutant, TO-336.rev, was able to replicate better than Matsuba.GMK3, but was still unable to elicit these responses. These data demonstrate that a high growth capacity at a high temperature is not necessarily critical for eliciting humoral immune responses in animals. In the view of the care and use of laboratory animals, it is desirable to replace the marker test by a test involving cultured cells. However, our data show that a test for the ts phenotype using cultured cells cannot be a substitute for the marker test using animals. The present data showed that a phenotypic reversion of the virus, by which TO-336.vac became able to grow at a high temperature, was insufficient to elicit humoral immune responses. These data suggest that TO-336.vac has one or more mutations that specifically abolish the potency to elicit these immune responses in animals. It is of interest that TO-336.vac has mutations in the E1 surface glycoprotein, because it is known to be involved in cell entry and induction of neutralizing and HI antibodies. Functional or antigenic changes to this surface glycoprotein may play a role in determining the potency of viruses to elicit humoral immune responses. Analyses of these mutations are in progress in our laboratory.

In summary, the entire nucleotide sequences of all the Japanese rubella vaccines became available with the data obtained in the present study. Nucleotide sequence analyses of progenitor RuV strains and their resulting vaccines revealed mutations that were introduced into the genomes of TO-336.vac and Matsuura.vac during their passages in laboratories. Among these, the N1159S mutation in the protease domain of P150 seems to affect the thermal stability of the protein. The data further suggested that a reduction in the thermal stability of the protease domain is a cause of the ts phenotype of some rubella vaccines. Finally, our data showed that the ability of RuV to grow at a high temperature was not necessarily correlated with the potency to elicit humoral immune responses in animals. These findings indicate that the molecular mechanisms underlying the inability of vaccines to elicit humoral responses in animals are more complicated than the hitherto considered mechanism involving the ts phenotype as the major cause.

Acknowledgments

We thank Drs. Y. Ami and Y. Suzaki, Division of Experimental Animal Research, for technical support with the marker test, Dr. M. Ochiai, Division of Quality Assurance, for useful comments about the statistical processing, and Drs. I. Kurane and M. Tashiro for their support and useful comments. We acknowledge all the members of our laboratory for helpful comments and technical support. This work was partly supported by grants from the Ministry of Health, Labour and Welfare of Japan.

References

[1] Hobman T, Chantler J. Rubella virus. In: Knipe DM, Howley PM, Griffin DE, Lamb RA, Martin MA, Roizman B, et al., editors. Fields virology. 5th ed. Philadelphia: Lippincott Williams & Wilkins; 2007. p. 1069–100.
[2] Gregg NM. Congenital cataract following German measles in the mother. Trans Ophthalmol Soc Aust 1941;3:35–46.
[3] Parkman PD, Buescher EL, Artenstein MS. Recovery of rubella virus from army recruits. Proc Soc Exp Biol Med 1962;111:225–30.
[4] Weller TH, Neva FA. Propagation in tissue culture of cytopathic agents form patients with rubella-like illness. Proc Soc Exp Biol Med 1962;111:215–25.
[5] Ohtawara M, Kobune F, Umino Y, Sugiura A. Inability of Japanese rubella vaccines to induce antibody response in rabbits is due to growth restriction at 39 °C. Arch Virol 1985;83(3–4):217–27.
[6] Shishido A, Ohtawara M. Development of attenuated rubella virus vaccines in Japan. Jpn J Med Sci Biol 1976;29(October (5)):227–53.
[7] Best JM. Rubella vaccines: past, present and future. Epidemiol Infect 1991;107(1):17–30.
[8] Association of biologicals manufactures of Japan. Minimum requirements for biological products. Tokyo, 1993.
[9] National Institute of Infectious Diseases. Minimum requirements for biological products; 2006 [cited; Available from: http://www.nih.go.jp/niid/MRBP/files/seibutsuki_english.pdf.
[10] Dominguez G, Wang CY, Frey TK. Sequence of the genome RNA of rubella virus: evidence for genetic rearrangement during togavirus evolution. Virology 1990;177(1):225–38.
[11] Pugachev KV, Abernathy ES, Frey TK. Genomic sequence of the RA27/3 vaccine strain of rubella virus. Arch Virol 1997;142(6):1165–80.
[12] Sakata M, Komase K, Nakayama T. Histidine at position 1042 of the p150 region of a KRT live attenuated rubella vaccine strain is responsible for the temperature sensitivity. Vaccine 2009;27(2):234–42.
[13] Kakizawa J, Nitta Y, Yamashita T, Ushijima H, Katow S. Mutations of rubella virus vaccine TO-336 strain occurred in the attenuation process of wild progenitor virus. Vaccine 2001;19(20–22):2793–802.
[14] Clarke DM, Loo TW, Hui I, Chong P, Gillam S. Nucleotide sequence and in vitro expression of rubella virus 24S subgenomic messenger RNA encoding the structural proteins E1,E2 and C. Nucleic Acids Res 1987;15(7):3041–57.
[15] W.H.O. Standardization of the nomenclature for genetic characteristics of wild-type rubella viruses. Wkly Epidemiol Rec 2005;80(14):126–32.
[16] Chen HH, Stark CJ, Atreya CD. The rubella virus nonstructural protease recognizes itself via an internal sequence present upstream of the cleavage site for trans-activity. Arch Virol 2006;151(9):1841–51.
[17] Frey TK. Molecular biology of rubella virus. Adv Virus Res 1994;44:69–160.
[18] Papps CL, Tzeng WP, Frey TK. Evaluation of cis-acting elements in the rubella virus subgenomic RNA that play a role in its translation. Arch Virol 2005;151(2):327–46.
[19] Katow S, Minahara H, Ota T, Fukushima M. Identification of strain-specific nucleotide sequences in E1 and NS4 genes of rubella virus vaccine strains in Japan. Vaccine 1997;15(14):1579–85.
[20] Zhou Y, Ushijima H, Frey TK. Genomic analysis of diverse rubella virus genotypes. J Gen Virol 2007;88(Pt 3):932–41.
[21] Koonin EV, Gorbalenya AE, Purdy MA, Rozanov MN, Reyes GR, Bradley DW. Computer-assisted assignment of functional domains in the nonstruc-

tural polyprotein of hepatitis E virus: delineation of an additional group of positive-strand RNA plant and animal viruses. Proc Natl Acad Sci USA 1992;89(17):8259–63.
[22] Rozanov MN, Koonin EV, Gorbalenya AE. Conservation of the putative methyltransferase domain: a hallmark of the 'Sindbis-like' supergroup of positive-strand R.N.A. viruses. J Gen Virol 1992;73(Pt 8):2129–34.
[23] Liang Y, Yao J, Gillam S. Rubella virus nonstructural protein protease domains involved in trans- and cis-cleavage activities. J Virol 2000;74(12):5412–23.
[24] Zhou Y, Tzeng WP, Wong HC, Ye Y, Jiang J, Chen Y, et al. Calcium-dependent association of calmodulin with the rubella virus nonstructural protease domain. J Biol Chem 2010;285(12):8855–68.
[25] Sutter RW, Kew OM, Cochi SL. Poliovirus vaccine-live. In: Plotkin SA, Orenstein WA, Offit PA, editors. Vaccines. 5 ed Elsevier; 2008. p. 631–85.
[26] Strebel PM, Papania MJ, Dayan GH, Halsey NA. Measles vaccine. In: Plotkin SA, Orenstein WA, Offit PA, editors. Vaccine. 5 ed Elsevier; 2008. p. 353–98.
[27] Plotkin SA, Rubin SA. Mumps vaccine. In: Plotkin SA, Orenstein WA, Offit PA, editors. Vaccine. 5 ed Elsevier; 2008. p. 435–65.
[28] Plotkin SA, Reef SE. Rubella vaccine. In: Plotkin SA, Orenstein WA, Offit PA, editors. Vaccine. 5 ed Elsevier; 2008. p. 735–71.
[29] Zhou Y, Tzeng WP, Yang W, Ye Y, Lee HW, Frey TK, et al. Identification of a Ca2+-binding domain in the rubella virus nonstructural protease. J Virol 2007;81(14):7517–28.
[30] Zhou Y, Tzeng WP, Ye Y, Huang Y, Li S, Chen Y, et al. A cysteine-rich metal-binding domain from rubella virus non-structural protein is essential for viral protease activity and virus replication. Biochem J 2009;417(2):477–83.
[31] Whitehead SS, Juhasz K, Firestone CY, Collins PL, Murphy BR. Recombinant respiratory syncytial virus (RSV) bearing a set of mutations from cold-passaged RSV is attenuated in chimpanzees. J Virol 1998;72(5):4467–71.
[32] Subbarao EK, Park EJ, Lawson CM, Chen AY, Murphy BR. Sequential addition of temperature-sensitive missense mutations into the PB2 gene of influenza A transfectant viruses can effect an increase in temperature sensitivity and attenuation and permits the rational design of a genetically engineered live influenza A virus vaccine. J Virol 1995;69(10):5969–77.
[33] Snyder MH, Betts RF, DeBorde D, Tierney EL, Clements ML, Herrington D, et al. Four viral genes independently contribute to attenuation of live influenza A/Ann Arbor/6/60 (H2N2) cold-adapted reassortant virus vaccines. J Virol 1988;62(2):488–95.
[34] Skiadopoulos MH, Surman S, Tatem JM, Paschalis M, Wu SL, Udem SA, et al. Identification of mutations contributing to the temperature-sensitive, cold-adapted, and attenuation phenotypes of the live-attenuated cold-passage 45 (cp45) human parainfluenza virus 3 candidate vaccine. J Virol 1999;73(2):1374–81.
[35] Skiadopoulos MH, Durbin AP, Tatem JM, Wu SL, Paschalis M, Tao T, et al. Three amino acid substitutions in the L protein of the human parainfluenza virus type 3 cp45 live attenuated vaccine candidate contribute to its temperature-sensitive and attenuation phenotypes. J Virol 1998;72(3):1762–8.
[36] Crowe Jr JE, Bui PT, Siber GR, Elkins WR, Chanock RM, Murphy BR. Cold-passaged, temperature-sensitive mutants of human respiratory syncytial virus (RSV) are highly attenuated, immunogenic, and protective in seronegative chimpanzees, even when RSV antibodies are infused shortly before immunization. Vaccine 1995;13(9):847–55.
[37] Hall SL, Stokes A, Tierney EL, London WT, Belshe RB, Newman FC, et al. Cold-passaged human parainfluenza type 3 viruses contain ts and non-ts mutations leading to attenuation in rhesus monkeys. Virus Res 1992;22(3):173–84.
[38] Juhasz K, Whitehead SS, Bui PT, Biggs JM, Crowe JE, Boulanger CA, et al. The temperature-sensitive (ts) phenotype of a cold-passaged (cp) live attenuated respiratory syncytial virus vaccine candidate, designated cpts530, results from a single amino acid substitution in the L protein. J Virol 1997;71(8):5814–9.
[39] Komase K, Nakayama T, Iijima M, Miki K, Kawanishi R, Uejima H. The phosphoprotein of attenuated measles AIK-C vaccine strain contributes to its temperature-sensitive phenotype. Vaccine 2006;24(6):826–34.
[40] Palese P. The genes of influenza virus. Cell 1977;10(1):1–10.
[41] Gombold JL, Estes MK, Ramig RF. Assignment of simian rotavirus SA11 temperature-sensitive mutant groups B and E to genome segments. Virology 1985;143(1):309–20.
[42] Sparks JS, Donaldson EF, Lu X, Baric RS, Denison MR. A novel mutation in murine hepatitis virus nsp5, the viral 3C-like proteinase, causes temperature-sensitive defects in viral growth and protein processing. J Virol 2008;82(12):5999–6008.
[43] Lulla V, Merits A, Sarin P, Kaariainen L, Keranen S, Ahola T. Identification of mutations causing temperature-sensitive defects in Semliki Forest virus RNA synthesis. J Virol 2006;80(6):3108–11.
[44] Suomalainen M, Garoff H, Baron MD. The E2 signal sequence of rubella virus remains part of the capsid protein and confers membrane association in vitro. J Virol 1990;64(11):5500–9.
[45] Yao J, Gillam S. Mutational analysis, using a full-length rubella virus cDNA clone, of rubella virus E1 transmembrane and cytoplasmic domains required for virus release. J Virol 1999;73(6):4622–30.

zjv00613/zjv7366d13z | xppws | S=1 | 1/16/13 | 5:21 | 4/C Fig: 1,2 | ArtID: 03029-12 | NLM: brief-report | CE: jtc

Editor: Garcia-Sastre | Section: Virus-Cell Interactions | Designation: S

JVI Journals.ASM.org

The Receptor-Binding Site of the Measles Virus Hemagglutinin Protein Itself Constitutes a Conserved Neutralizing Epitope

AQ: au Maino Tahara,[a] Shinji Ohno,[b] Kouji Sakai,[a] Yuri Ito,[c] Hideo Fukuhara,[c] Katsuhiro Komase,[a] Melinda A. Brindley,[d] Paul A. Rota,[e] Richard K. Plemper,[d] Katsumi Maenaka,[c] Makoto Takeda[a]

Department of Virology 3, National Institute of Infectious Diseases, Tokyo, Japan[a]; Department of Virology, Faculty of Medicine, Kyushu University, Fukuoka, Japan[b]; Laboratory of Biomolecular Science, Faculty of Pharmaceutical Sciences, Hokkaido University, Hokkaido, Japan[c]; Department of Pediatrics, Emory University School of Medicine, Atlanta, Georgia, USA[d]; Measles, Mumps, Rubella and Herpesviruses Laboratory Branch, Division of Viral Diseases, Centers for Disease Control and Prevention, Atlanta, Georgia, USA[e]

Here, we provide direct evidence that the receptor-binding site of measles virus (MV) hemagglutinin protein itself forms an effective conserved neutralizing epitope (CNE). Several receptor-interacting residues constitute the CNE. Thus, viral escape from neutralization has to be associated with loss of receptor-binding activity. Since interactions with both the signaling lymphocyte activation molecule (SLAM) and nectin4 are critical for MV pathogenesis, its escape, which results from loss of receptor-binding activity, should not occur in nature.

Measles virus (MV) is an enveloped virus that belongs to the genus *Morbillivirus* of the family *Paramyxoviridae* and possesses two types of surface glycoprotein spikes, the hemagglutinin (H) and fusion (F) proteins. MV infection is initiated by binding of the H protein to cellular receptors on the target host cells. The binding triggers membrane fusion between the virus envelope and the host cell plasma membrane mediated by the F protein. The signaling lymphocyte activation molecule (SLAM) on a subset of immune cells and nectin4 at adherens junctions are the principal receptors for MV (1–4). The H and F proteins are both neutralizing targets, but greater amounts of antibodies (Abs) are elicited against the H protein than the F protein, and the H protein-specific antibodies mainly contribute to neutralization of MV infection *in vivo* (5–8). All the available data suggest that measles eradication is biologically feasible (9, 10), and one of the major factors that would ensure measles eradication is the single-serotype nature of MV. Our previous paper suggested that the receptor-binding site (RBS) on the H protein, which is exposed outside the heavy N-glycan shields, may constitute a major neutralizing epitope that contributes to the single-serotype nature of MV (11). However, our recent paper (12) showing the detailed locations of five epitopes (*I*, *II*, *iv*, *v*, and *vi*) on the H protein provided insufficient evidence that the RBS acts as a neutralizing epitope. Here, we provide direct and concrete evidence that the RBS itself forms an effective conserved neutralizing epitope (CNE) which provides a strong functional constraint against change.

In the present study, we characterized a new mouse monoclonal antibody (MAb), 2F4. MAb 2F4 was produced using a cell line expressing the H protein of the wild-type IC-B strain as an antigen. For competitive binding enzyme-linked immunosorbent assays (cELISAs), MV antigens precoated on cELISA plates (Denka Seiken) were incubated with previously reported MAbs (E81, E128, E185, E39, and E103) (12, 13), 2F4 or phosphate-buffered saline for 1 h and then incubated with MAb 2F4 labeled with biotin using a biotin labeling kit (NH2; Dojindo Laboratories). After three washes, the MV antigens bound by the MAbs were incubated with a streptavidin-horseradish peroxidase (HRP) conjugate (Thermo Scientific) for 1 h before addition of the TMB substrate (3,3′5,5′-tetramethylbenzidine; Denka Seiken). The plates were incubated for 25 min, and the colorimetric reactions were stopped by addition of H_2SO_4. The optical density (OD) values were analyzed using a microplate reader (Bio-Rad). The data revealed that binding of 2F4 was not inhibited by MAbs recognizing epitopes *I*, *iv*, *v*, and *vi* (E81, E185, E39, and E103, respectively) (12) (Table 1; the epitope recognized by 2F4 is tentatively termed epitope *vii*). On the other hand, E128 recognizing epitope *II* (12) showed partial inhibition of 2F4 binding (Table 1). Epitope *II* is shielded by the N-glycan modification at amino acid position 416 (N416-sugar), and viruses with the N416-sugar (genotypes D3, D4, D5, and D9 among the eight genotypes) are not neutralized by E128 (12). Eight distinct recombinant MVs (rMVs) encoding a *Renilla* luciferase reporter gene and an H gene derived from different MV genotypes (A, B3, D3, D4, D5, D8, D9, and H1) were used as neutralization targets for 2F4 (Table 2), as reported previously (12). The data clearly demonstrated that, unlike E128 recognizing epitope *II*, 2F4 showed high neutralizing titers against all eight rMVs (Table 2). These data suggested that epitope *vii* is a CNE and is distinct from all the other five epitopes (*I*, *II*, *iv*, *v*, and *vi*).

AQ: A/T1 T2

When the H protein-SLAM interaction was assessed by surface plasmon resonance assays, as reported previously (12), MAb 2F4 blocked binding of the H protein to SLAM, as did MAbs B5 and E128 recognizing epitopes *I* and *II*, which are located near the RBS (12) (Table 3). These data suggest that epitope *vii* is located at or near the RBS. A panel of rMVs possessing amino acid substitutions at the RBS were analyzed for neutralization by 2F4. On the D3 genetic background (IC323 strain [14]), four rMVs encoding enhanced green fluorescent protein (EGFP) and possessing mutations at a SLAM-interacting residue (R533A) (Fig. 1B) and nectin4-interacting residues (F483A, Y543S, and S544A/Y541S) (Fig.

T3 F1

Received 29 October 2012 Accepted 26 December 2012
Published ahead of print 2 January 2013
Address correspondence to Maino Tahara, maino@nih.go.jp.

doi:10.1128/JVI.03029-12

TABLE 1 Summary of competitive binding ELISAs of anti-H protein MAbs

Unlabeled MAb	Antigenic site	Biotinylated MAb 2F4 (*vii*) inhibition[a]
E81	*I*	−
E128	*II*	+
E185	*iv*	−
E39	*v*	−
E103	*vi*	−
2F4	*vii*	++

[a] ++, complete inhibition; +, partial inhibition; −, no inhibition.

1C) (15–19) were generated and assessed for virus spreading in SLAM-positive (SLAM$^+$) B95a and nectin4$^+$ II-18 cells (20) in the presence or absence of 2F4 (Fig. 2). The rMVs with F483A and Y543S were reported previously (15). As shown in Fig. 2, in the absence of 2F4 [Ab(−)], wild-type MV spread efficiently in both cell types using SLAM or nectin4. On the other hand, rMVs with F483A, Y543S, or S544A/Y541S lost the ability to use nectin4 as a receptor and thus failed to spread in II-18 cells, even in the absence of 2F4. Similarly, rMV with R533A lost the ability to use SLAM as a receptor and did not spread in B95a cells. However, in the presence of 2F4, the mutant MVs showed advantages for spreading. Even in the presence of 2F4, rMVs with F483A, Y543S, or S544A/Y541S were able to spread in SLAM$^+$ B95a cells, and rMV with R533 was able to spread in nectin4$^+$ II-18 cells, whereas the wild-type MV infection was completely neutralized by 2F4. Similar experiments were performed using luciferase-expressing rMVs (21). Two rMVs with mutations at SLAM-interacting residues (D505S and R533A) (17, 19) (Fig. 1B) and two rMVs with mutations at nectin4-interacting residues (F483A and Y543S) (15, 16, 18) (Fig. 1C) were generated (rMVs with F483A and Y543S were reported previously [15]). In part, as reported previously, rMVs with F483A (15) and Y543S (15) were unable to bind to nectin4 (2, 3), and those with R533A (16) and D505S (in the present study) lost the ability to use SLAM (Table 4). Meanwhile, the F483A, Y543S, D505S, and R533A substitutions all resulted in escape from neutralization by 2F4 (Table 4). These data demonstrated that the RBS used for interactions with both SLAM and nectin4 constitutes epitope *vii* recognized by 2F4 (Fig. 1). Consequently, MV escape

TABLE 2 Neutralizing titers against MV strains possessing H genes from different genotypes

Cell line	Genotype, yr isolated	Neutralizing titer)[a] 2F4 (*vii*)	E128 (*II*)[b]
B95a	A, 1954	22,141	1,968
	B3, 2009	11,070	1,968
	D3, 1984	22,141	15
	D4, 2009	22,141	31
	D5, 2001	11,070	15
	D8, 2009	44,281	1,968
	D9, 2010	11,070	15
	H1, 2009	22,141	1,968
II-18	A, 1954	11,070	62,977
	B3, 2009	11,070	62,977
	D3, 1984	11,070	123
	D4, 2009	11,070	31
	D5, 2001	22,141	<4
	D8, 2009	22,141	62,977
	D9, 2010	11,070	123
	H1, 2009	22,141	62,977

[a] Data represent neutralizing titers for 1 mg/ml of immunoglobulin.
[b] Data for E128 are taken from reference 12.

TABLE 3 Competitive binding of anti-H protein MAbs against SLAM[a]

MAb	Antigenic site	Competitive activity[b]
2F4	*vii*	++
B5	*I*	++
E128	*II*	++
E103	*vi*	−

[a] The detailed procedure has been previously reported (12).
[b] ++, complete inhibition; −, no inhibition.

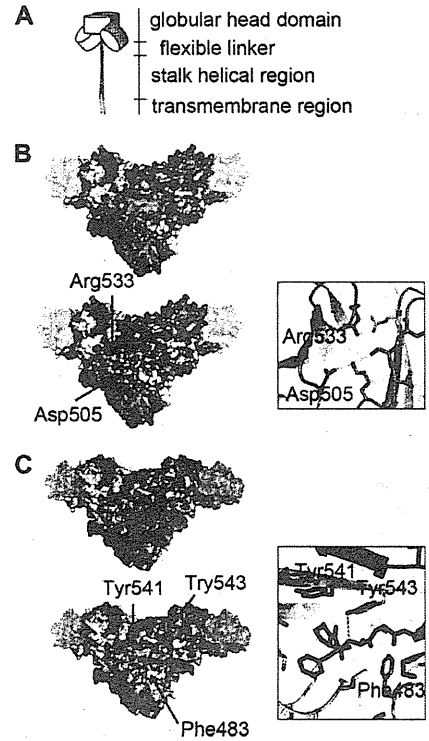

FIG 1 Location of epitope *vii* on the H protein tetrameric structure. (A) Diagram of an H protein tetramer (a dimer of H protein dimers). The four H protein molecules are shown in dark gray, light gray, dark purple, and light purple. (B) Location of SLAM-interacting residues, which constitute epitope *vii* on the tetrameric H protein structure in complex with SLAM (19). SLAM is shown in translucent cyan. SLAM interacting with the gray H protein is deleted in the structure shown at the bottom. A detailed view in a ribbon and stick diagram is shown in the box. SLAM is shown in cyan, and H protein is shown in orange or yellow. (C) Location of nectin4-interacting residues, which constitute epitope *vii*. The tetrameric structure was reconstructed using data by Hashiguchi et al. (19) and Zhang et al. (18). Nectin4 is shown in translucent magenta. Nectin4 interacting with the gray H protein is deleted in the structure shown at the bottom. A detailed view in a ribbon and stick diagram is shown in the box. Nectin4 is shown in magenta, and H protein is shown in orange or yellow. (B and C) The figures were produced using PyMOL (Schrödinger; http://www.pymol.org). The amino acid residues demonstrated or suggested to constitute portions of epitopes are shown in colors as follows: residues on beta-sheets 1, 2, 3, 4, 5, and 6 (19) are shown in blue, dark green, light green, yellow, orange, and red, respectively.

COLOR

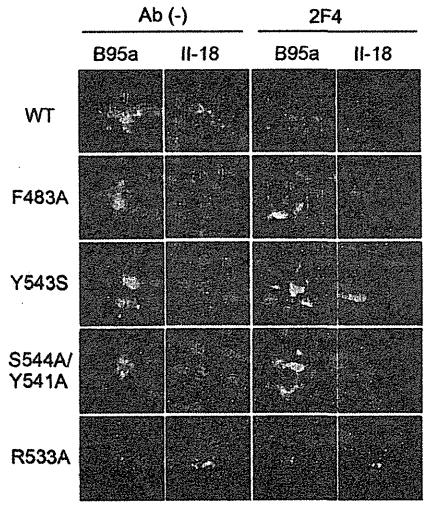

COLOR

FIG 2 Effects of specific substitutions on virus infectivity and MAb neutralization. EGFP autofluorescence in MV-infected SLAM$^+$ B95a cells and nectin4$^+$ II-18 cells is shown. B95a and II-18 cells were infected with rMVs containing F483A, Y543S, S544A/Y541S, and R533A substitutions in the presence or absence of MAb 2F4. The panels show representative images observed using a fluorescence microscope.

from neutralization by 2F4 is penalized by loss of affinity for one of the principal MV receptors.

Apparently, a previously reported MAb, I-41, also recognizes this *vii* epitope (22), since a substitution at position 552 (the phenylalanine at this position is predicted to interact with SLAM [19]) allowed MV to escape from neutralization. Another previous study implied that MAb 80-II-B2 recognizes a region containing residues 505 and 506 within this epitope (23). The H protein of the CAM-70 MV vaccine strain features a mutation at position 505. Accordingly, the CAM-70 vaccine strain does not react with 80-II-B2 and binds to SLAM inefficiently (23, 24). Previous competitive binding studies revealed that MAb 16-DE6 recognizes the same antigenic site as I-41 (25), and that an 16-DE6 escape mutant contained, among other changes, an arginine-to-glycine substitution at position 533 (R533G) (22). Previously characterized MAbs

TABLE 4 Neutralizing titers against recombinant MVs possessing the IC-H protein with various amino acid substitutions

Cell line	Mutation	Infectivity	Neutralizing titer[a]			
			B5 (*I*)	E81 (*I*)	E103 (*vi*)	2F4 (*vii*)
B95a	Wild type (−)	+	7,536	1,727	10,231	22,141
	F483A	+	3,768	1,727	10,231	<346
	Y543S	+	1,884	1,727	2,558	692
	D505S	−	NA	NA	NA	NA
	R533A	−	NA	NA	NA	NA
II-18	Wild type (−)	+	3,764	27,631	20,462	11,070
	F483A	−	NA	NA	NA	NA
	Y543A	−	NA	NA	NA	NA
	D505S	+	1,884	13,815	20,462	<5
	R533A	+	1,884	27,631	20,462	173

[a] Data represent neutralizing titers for 1 mg/ml of immunoglobulin. NA, not applicable.

B2 and BH26 similarly recognize this epitope (6, 25, 26), which appears to be a premier neutralizing epitope for the H protein. Residues located in this epitope may be involved in SLAM-binding activity (6, 26). Therefore, this region probably corresponds to epitope *vii* identified in our study.

In summary, the present data demonstrate that both the SLAM- and nectin4-interacting residues themselves constitute a CNE. Since these residues are critical for interaction with either SLAM or nectin4, viral escape from neutralization has to be associated with loss of the receptor-binding activity. Since efficient MV spreading mandates interactions of the H protein with these two discrete proteinaceous receptors, SLAM and nectin4 (4), residues within this domain are likely to be under high selective pressure to maintain their molecular identity, and contribute to the sustainability of the single-serotype nature of MV.

ACKNOWLEDGMENTS

We thank T.A. Sato, Y. Yanagi, and T. Seya for providing MAbs, N. Ito and M. Sugiyama for providing BHK/T7-9 cells, and K. Taira for providing an MV isolate. We also thank all the members of Department of Virology 3, NIID, Japan, for technical support.

REFERENCES

1. Tatsuo H, Ono N, Tanaka K, Yanagi Y. 2000. SLAM (CDw150) is a cellular receptor for measles virus. Nature 406:893–897.
2. Noyce RS, Bondre DG, Ha MN, Lin LT, Sisson G, Tsao MS, Richardson CD. 2011. Tumor cell marker PVRL4 (nectin 4) is an epithelial cell receptor for measles virus. PLoS Pathog. 7:e1002240. doi:10.1371/journal.ppat.1002240.
3. Mühlebach MD, Mateo M, Sinn PL, Prufer S, Uhlig KM, Leonard VH, Navaratnarajah CK, Frenzke M, Wong XX, Sawatsky B, Ramachandran S, McCray PB, Jr, Cichutek K, von Messling V, Lopez M, Cattaneo R. 2011. Adherens junction protein nectin-4 is the epithelial receptor for measles virus. Nature 480:530–533.
4. Takeda M, Tahara M, Nagata N, Seki F. 2011. Wild-type measles virus is intrinsically dual-tropic. Front. Microbiol. 2:279. doi:10.3389/fmicb.2011.00279.
5. de Swart RL, Yuksel S, Osterhaus AD. 2005. Relative contributions of measles virus hemagglutinin- and fusion protein-specific serum antibodies to virus neutralization. J. Virol. 79:11547–11551.
6. Bouche FB, Ertl OT, Muller CP. 2002. Neutralizing B cell response in measles. Viral Immunol. 15:451–471.
7. de Swart RL, Yuksel S, Langerijs CN, Muller CP, Osterhaus AD. 2009. Depletion of measles virus glycoprotein-specific antibodies from human sera reveals genotype-specific neutralizing antibodies. J. Gen. Virol. 90:2982–2989.
8. Duke T, Mgone CS. 2003. Measles: not just another viral exanthem. Lancet 361:763–773.
9. Sanders R, Dabbagh A, Featherstone D. 2011. Risk analysis for measles reintroduction after global certification of eradication. J. Infect. Dis. 204(Suppl 1):S71–S77.
10. Bellini WJ, Rota PA. 2011. Biological feasibility of measles eradication. Virus Res. 162:72–79.
11. Hashiguchi T, Kajikawa M, Maita N, Takeda M, Kuroki K, Sasaki K, Kohda D, Yanagi Y, Maenaka K. 2007. Crystal structure of measles virus hemagglutinin provides insight into effective vaccines. Proc. Natl. Acad. Sci. U. S. A. 104:19535–19540.
12. Tahara M, Ito Y, Brindley MA, Ma X, He J, Xu S, Fukuhara H, Sakai K, Komase K, Rota PA, Plemper RK, Maenaka K, Takeda M. 2013. Functional and structural characterization of neutralizing epitopes of measles virus hemagglutinin protein. J. Virol. 87:666–675.
13. Sato TA, Fukuda A, Sugiura A. 1985. Characterization of major structural proteins of measles virus with monoclonal antibodies. J. Gen. Virol. 66(Pt 7):1397–1409.
14. Takeda M, Takeuchi K, Miyajima N, Kobune F, Ami Y, Nagata N, Suzaki Y, Nagai Y, Tashiro M. 2000. Recovery of pathogenic measles virus from cloned cDNA. J. Virol. 74:6643–6647.
15. Tahara M, Takeda M, Shirogane Y, Hashiguchi T, Ohno S, Yanagi Y.

2008. Measles virus infects both polarized epithelial and immune cells by using distinctive receptor-binding sites on its hemagglutinin. J. Virol. 82: 4630–4637.

16. Leonard VH, Sinn PL, Hodge G, Miest T, Devaux P, Oezguen N, Braun W, McCray PB, McChesney MB, Cattaneo R. 2008. Measles virus blind to its epithelial cell receptor remains virulent in rhesus monkeys but cannot cross the airway epithelium and is not shed. J. Clin. Invest. 118:2448–2458.
17. Vongpunsawad S, Oezgun N, Braun W, Cattaneo R. 2004. Selectively receptor-blind measles viruses: identification of residues necessary for SLAM- or CD46-induced fusion and their localization on a new hemagglutinin structural model. J. Virol. 78:302–313.
18. Zhang X, Lu G, Qi J, Li Y, He Y, Xu X, Shi J, Zhang C, Yan J, Gao GF. 2013. Structure of measles virus hemagglutinin bound to its epithelial receptor nectin-4. Nat. Struct. Mol. Biol. 20:67–72.
19. Hashiguchi T, Ose T, Kubota M, Maita N, Kamishikiryo J, Maenaka K, Yanagi Y. 2011. Structure of the measles virus hemagglutinin bound to its cellular receptor SLAM. Nat. Struct. Mol. Biol. 18:135–141.
20. Shirogane Y, Takeda M, Tahara M, Ikegame S, Nakamura T, Yanagi Y. 2010. Epithelial-mesenchymal transition abolishes the susceptibility of polarized epithelial cell lines to measles virus. J. Biol. Chem. 285:20882–20890.
21. Takeda M, Ohno S, Tahara M, Takeuchi H, Shirogane Y, Ohmura H, Nakamura T, Yanagi Y. 2008. Measles viruses possessing the polymerase protein genes of the Edmonston vaccine strain exhibit attenuated gene expression and growth in cultured cells and SLAM knock-in mice. J. Virol. 82:11979–11984.
22. Hu A, Sheshberadaran H, Norrby E, Kovamees J. 1993. Molecular characterization of epitopes on the measles virus hemagglutinin protein. Virology 192:351–354.
23. Hummel KB, Bellini WJ. 1995. Localization of monoclonal antibody epitopes and functional domains in the hemagglutinin protein of measles virus. J. Virol. 69:1913–1916.
24. Kato S, Ohgimoto S, Sharma LB, Kurazono S, Ayata M, Komase K, Takeda M, Takeuchi K, Ihara T, Ogura H. 2009. Reduced ability of hemagglutinin of the CAM-70 measles virus vaccine strain to use receptors CD46 and SLAM. Vaccine 27:3838–3848.
25. Sheshberadaran H, Norrby E. 1986. Characterization of epitopes on the measles virus hemagglutinin. Virology 152:58–65.
26. Ertl OT, Wenz DC, Bouche FB, Berbers GA, Muller CP. 2003. Immunodominant domains of the Measles virus hemagglutinin protein eliciting a neutralizing human B cell response. Arch. Virol. 148:2195–2206.

SUPPLEMENT ARTICLE

Genetic Characterization of Measles Vaccine Strains

Bettina Bankamp,[1] Makoto Takeda,[2] Yan Zhang,[3] Wenbo Xu,[3] and Paul A. Rota[1]

[1]Division of Viral Diseases, Centers for Disease Control and Prevention, Atlanta; [2]Department of Virology III, National Institute of Infectious Diseases, Tokyo, Japan; and [3]National Institute for Viral Disease Control and Prevention, China Centers for Disease Control and Prevention, Bejing, China

The complete genomic sequences of 9 measles vaccine strains were compared with the sequence of the Edmonston wild-type virus. AIK-C, Moraten, Rubeovax, Schwarz, and Zagreb are vaccine strains of the Edmonston lineage, whereas CAM-70, Changchun-47, Leningrad-4 and Shanghai-191 were derived from 4 different wild-type isolates. Nucleotide substitutions were found in the noncoding regions of the genomes as well as in all coding regions, leading to deduced amino acid substitutions in all 8 viral proteins. Although the precise mechanisms involved in the attenuation of individual measles vaccines remain to be elucidated, in vitro assays of viral protein functions and recombinant viruses with defined genetic modifications have been used to characterize the differences between vaccine and wild-type strains. Although almost every protein contributes to an attenuated phenotype, substitutions affecting host cell tropism, virus assembly, and the ability to inhibit cellular antiviral defense mechanisms play an especially important role in attenuation.

Measles is a highly contagious disease characterized by fever, malaise, coryza, conjunctivitis, cough, and an erythematous maculopapular rash [1]. Although most patients recover from the illness, serious complications can occur, including pneumonia and invasion of the central nervous system [2, 3]. One severe complication is subacute sclerosing panencephalitis (SSPE), a rare, fatal consequence of central nervous system infection [4]. Measles caused an estimated 164,000 deaths worldwide in 2008 [5]. This number represents a 97% decrease from the estimated 6 million deaths occurring annually before the introduction of measles vaccines [6].

Measles virus (MeV) was first isolated from a child with measles in a primary culture of human kidney cells [7]. This isolate, the prototype Edmonston strain, was subsequently adapted to various types of cultured cells, giving rise to several of the currently used highly attenuated, live measles vaccines [8]. The first live, attenuated vaccine, Edmonston B, was licensed in the United States under the trade name Rubeovax in 1963 [9]. It was eventually replaced by the more attenuated Moraten strain [10]. On the basis of phylogenetic analyses, MeV isolates can be assigned to 1 of 23 recognized genotypes and 1 provisional genotype [11, 12]. All vaccine strains are grouped in genotype A, possibly because genotype A was the most widely distributed genotype at the time of isolation of the vaccines' wild-type progenitors [13].

MOLECULAR BIOLOGY OF MeV

MeV, an enveloped virus with a single-stranded, negative sense RNA genome, is a member of the genus *Morbillivirus* in the family *Paramyxoviridae* (for review see [2]). The genome is a 15,894-nucleotide, nonsegmented RNA molecule of negative polarity. It contains 6 transcription units which are separated by nontranscribed intergenic sequences consisting of 3 nucleotides. The 6 genes (Figure 1) encode 8 proteins. In addition to the 6

Potential conflicts of interest: none reported.

Supplement sponsorship: This article is part of a supplement entitled "Global Progress Toward Measles Eradication and Prevention of Rubella and Congenital Rubella Syndrome," which was sponsored by the Centers for Disease Control and Prevention.

Disclaimer: The findings and conclusions in this article are those of the authors and do not necessarily represent the views of the Centers for Disease Control and Prevention.

Correspondence: Bettina Bankamp, PhD, Div of Viral Diseases, Centers for Disease Control and Prevention, 1600 Clifton Road, MS C-22, Atlanta, GA 30333 (bbankamp@cdc.gov).

The Journal of Infectious Diseases 2011;204:S533–S548
Published by Oxford University Press on behalf of the Infectious Diseases Society of America 2011.
0022-1899 (print)/1537-6613 (online)/2011/204S1-0068$14.00
DOI: 10.1093/infdis/jir097

structural proteins described in Figure 1, 2 nonstructural proteins are encoded by the gene for the phosphoprotein (P). The C protein is translated from an overlapping reading frame in the P gene [14], whereas the V protein is the product of an edited mRNA transcribed from the P gene [15]. The edited message has a nontemplated G residue inserted at genomic nucleotide 2499. As a result, P and V share an amino-terminal domain of 231 amino acids but have unique carboxyl terminal domains of 276 and 69 amino acids, respectively.

The Functions of the MeV Proteins

The most abundant structural polypeptide, the nucleoprotein (N; 525 amino acids), is essential for packaging the genome into a ribonucleoprotein complex (RNP) that serves as a template for transcription, replication and is packaged into progeny virions [2]. The amino-terminal region of the N protein (N_{CORE}; amino acids 1–400) forms the core of the helical nucleocapsid, whereas the carboxyl-terminal region (N_{TAIL}; amino acids 401–525) constitutes a disordered domain located outside of the core [16]. This region is hypervariable among wild-type viruses, and the nucleotide sequence of this region is used for genotype assignation [17, 18]. The N_{TAIL} region interacts with the P protein [19, 20] and the M protein [21]. Two leucine residues at amino acid positions 523 and 524 are required for the interaction with the M protein [21]. The N protein also interacts with multiple cellular proteins [22–25]. The major inducible 70-kDa heat shock protein, hsp72, promotes MeV RNA synthesis and virus propagation by interacting with the N_{TAIL} region [26–28]. An asparagine residue at amino acid position 522 (Asn522) in the N_{TAIL} region is important for the interaction with hsp72 [29].

The phosphoprotein (P; 507 amino acids) is a subunit of the viral RNA polymerase and acts as a chaperone that interacts with and regulates the cellular localization of N protein and probably assists in nucleocapsid assembly [20, 30, 31]. The P protein forms oligomers and binds the N protein and the polymerase protein. A domain in the amino-terminus of P is required for interactions with soluble N protein, whereas the unique carboxyl-terminus contains the self-assembly domain and binding sites for the nucleocapsid and the polymerase [2, 20, 30, 32]. The P, V (299 amino acids), and C (186 amino acids) proteins all play roles in antagonizing the host interferon (IFN) responses [33]. The V protein blocks the Jak/STAT signaling pathway and counteracts cellular IFN signaling [34–39]. It also blocks the MDA5-mediated IFN induction pathway [40–42]. Direct interference with IFN signaling by the P and C proteins has also been reported [36, 43, 44]. The C protein controls the levels of viral RNA synthesis [45, 46] to circumvent IFN induction [35, 42, 47]. The V protein binds RNA and can also regulate viral RNA synthesis [48, 49].

The matrix protein (M; 335 amino acids) lines the inner surface of the viral envelope and participates in virion maturation [2, 50]. It plays a crucial role in virus assembly by interacting with the cytoplasmic tails of the H and F proteins [51–53]. It binds the nucleocapsid and negatively regulates transcription, presumably by sequestering nucleocapsids to the plasma membrane [21, 54, 55].

The fusion protein (F) is translated as a precursor of 550 amino acids that is cleaved by cellular furin-like proteases into disulfide-linked F1 and F2 proteins. It is a cell surface–expressed, type I glycoprotein that mediates fusion with the host cell at neutral pH [2, 56].Three N-linked glycosylation sites are located in the F2 protein at amino acids 29, 61, and 67 [57]. Amino acids 113–145, located at the new amino-terminus of F1, form the hydrophobic fusion peptide [58]. This domain inserts into the membrane of the host cell during the fusion process [59]. A cytoplasmic tail of 33 amino acids at the carboxyl terminus of

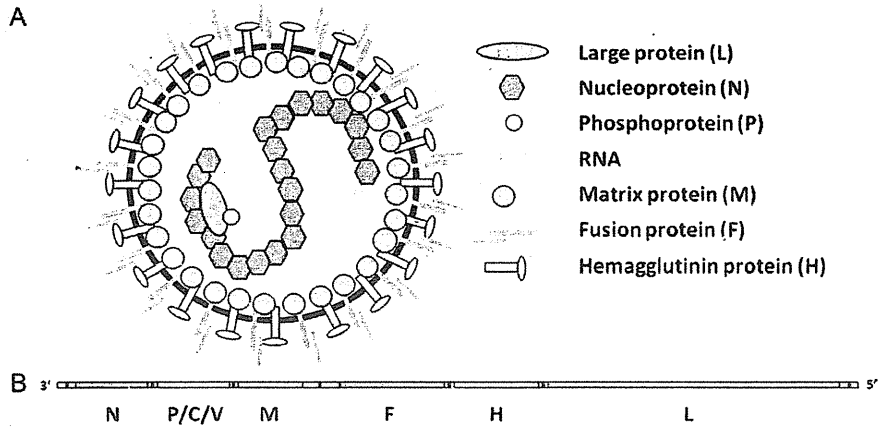

Figure 1. Measles virion and genome. *A*, Schematic representation of a measles virion. *B*, Organization of the measles genome. Colored rectangles represent coding regions, and white rectangles represent noncoding regions. Vertical black bars represent intergenic trinucleotides The size of the individual regions is not to scale.

F1 interacts with the M protein and contains sorting signals for intracellular localization [60].

The hemagglutinin (H; 617 amino acids) protein is the second glycosylated surface-expressed protein. This type 2 glycoprotein mediates attachment to specific protein receptors on the host cell and is a required co-factor for fusion [2]. There are 4 N-linked glycosylation sites between amino acids 168 and 200 [61], and some wild-type isolates are additionally glycosylated at amino acid 416 [62]. A cytoplasmic tail of 34 amino acids at the amino-terminus interacts with the M protein and contains sorting signals for intracellular localization [63, 64]. Two receptors have been identified for MeV [65]. hSLAM (human signaling lymphocyte activation molecule, CD150) is a common receptor for all MeV strains [66], whereas CD46 (membrane cofactor protein, MCP) functions as a receptor for vaccines and some laboratory-adapted strains, but not for wild-type strains [67, 68]. hSLAM is only expressed on a subset of immune cells [69–71]. All vaccine strains have acquired the ability to use CD46 as an alternative receptor during passage in various SLAM-negative cultured cells [65]. The ubiquitous expression of CD46 explains the ability of vaccine strains to infect various human and monkey cell lines. Recent studies have revealed that another, presently unidentified receptor exists for wild-type MeV on epithelial cells that form tight junctions (polarized epithelial cells) [72–76], and this as-yet uncharacterized receptor is referred to as "EpiR" in this review. The H protein is the major target for neutralizing antibodies induced by vaccination [77].

The Large gene encodes the multifunctional catalytic subunit of the RNA dependent RNA polymerase (L; 2183 amino acids), which is responsible for both transcription and replication [2, 31]. It is thought to carry out most (if not all) enzymatic activities required for transcription and replication, including nucleotide polymerization, mRNA capping, and polyadenylation [78–80]. On the basis of amino acid sequence conservation among nonsegmented negative strand viruses, 6 domains of higher conservation have been characterized in the L protein [81]. Within these domains, several functional motifs have been identified. The conserved domains may represent concatenated functional domains that are connected by less-conserved hinge regions [81]. L forms oligomers and binds its co-factor, the P protein. Binding sites for these interactions have been identified [82, 83]. Together with the genome, the N, P, and L proteins constitute the transcriptionally active RNP.

The Roles of Noncoding Regions

Nearly 11% of the 16-kb MeV genome is composed of noncoding RNA (Figure 1). The 6 transcription units are preceded by a 3′ leader and are followed by a 5′ trailer. All cis-acting regulatory elements such as promoters and encapsidation signals are contained within the first 107 and the last 109 nucleotides of the genome [84, 85]. Each gene contains 5′ and 3′ noncoding regions with conserved start and end signals for transcription and polyadenylation [86]. Morbillivirus genomes are unique within the *Paramyxoviridae* in that they contain a very long noncoding region of ~1000 nucleotides between the M and F open-reading frame (ORF) [56, 87]. The region is GC rich and is likely to fold into complex secondary RNA structures. The function of this region is not well understood, but it may play a role in regulating transcription of the M and F gene [88–90].

Measles Virus Replication

MeV attaches to the host cell through the interaction of the viral H protein with a cellular receptor that may be hSLAM, CD46 or the as-yet unidentified EpiR [65]. After the F protein mediates fusion of the virion with the cell membrane, the negative-stranded RNP is introduced into the cytoplasm, where it acts as a template for both primary transcription of mRNAs and replication into positive-stranded antigenomic RNA (for a review, see Lamb and Parks [91]). The polymerase complex, consisting of L and P proteins, is delivered with the RNP. mRNA transcripts are capped, polyadenylated and terminated at the gene end signals [92]. The full-length positive sense antigenomic intermediate acts as a template for the replication of full-length, negative sense genomic RNA. During replication the gene end, intergenic trinucleotide and gene start signals are ignored, and both nascent positive and negative sense genomes are concomitantly encapsidated to produce RNPs [93]. F and H proteins insert into the plasma membrane, whereas M proteins line the inside of the membrane and interact with the cytoplasmic tails of the glycoproteins and the RNP [50, 52]. The virion buds from the plasma membrane to complete the replication cycle.

ORIGINS AND PASSAGE HISTORIES OF VACCINE STRAINS

The first complete genomic sequence of a live, attenuated measles vaccine strain was published 1993 for the strain AIK-C [94] and was later updated by Parks et al [95, 96]. Since then, the genomic sequences of 8 additional vaccine strains have become available from GenBank (for accession numbers, see Figure 3). Sequence data were reanalyzed for this review; however, many of the findings were previously published [95–98]. Figure 2 summarizes the passage histories of the measles vaccines. Several of these strains were developed from the Edmonston isolate [7], whereas others were derived from wild-type progenitors isolated independently in Russia (Leningrad-4), Japan (CAM-70), and China (Shanghai-191) [99–101]. Unfortunately, the original Edmonston isolate is no longer available for analysis. Instead, vaccine sequences are compared with the Edmonston wild-type strain, which has undergone 13 passages in cell culture [8]. The AIK-C strain is used in Japan [102], where it was developed from the Edmonston strain [103]. The Zagreb strain (also referred to

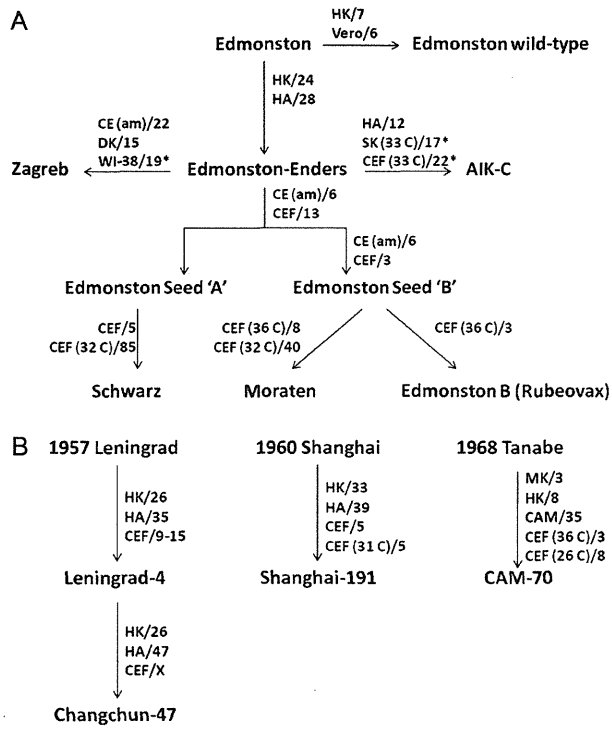

Figure 2. Passage histories (adapted from [8], with permission). *A*, Passage histories of Edmonston-derived vaccines. *B*, Passage histories of non–Edmonston-derived vaccines. Temperature of passages was assumed to be 37°C unless otherwise stated. A forward slash followed by a number indicates the number of passages. CAM, chorioallantoic cavity of chick embryo; CE(am), intraamniotic cavity of chick embryo; CEF, chick embryo fibroblast; DK, dog kidney; HA, human amnion; HK, human kidney; SK, sheep kidney; WI-38, human diploid cells; *Plaque purification.

as Edmonston-Zagreb) was derived from the Edmonston strain by further passaging and plaque purification in human diploid cells [104, 105]. It is produced by the Serum Institute of India and is the most commonly used measles vaccine in the

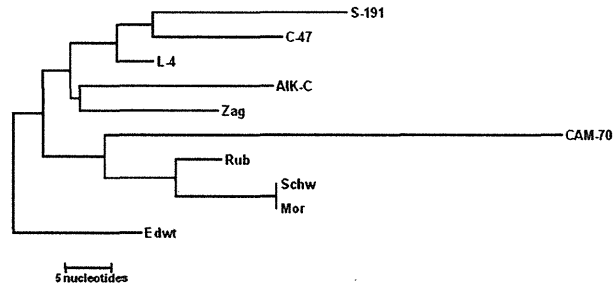

Figure 3. Phylogenetic tree based on complete genomic sequence for all vaccine strains. GenBank accession numbers are as follows: AF266288 (Edmonston wild-type, Edwt), AF266290 (Zagreb, Zag), AF266286 (AIK-C), AF266291 (Schwarz, Sch), AF266287 (Moraten, Mor), AF266289 (Rubeovax, Rub), FJ416068 (Changchun-47, C - 47), FJ416067 (Shanghai-191, S - 191), and DQ345723 (CAM-70). The tree was generated with MEGA4 [106] using maximum parsimony.

Expanded Programme on Immunization of the World Health Organization [107]. Edmonston B (Rubeovax) was developed from the Edmonston isolate by passaging in primary human and avian cell culture systems [108–111]. Although the vaccine induced excellent seroconversion rates, it also induced fever in 46% of vaccinees [9] and was replaced with further attenuated strains [9]. The Schwarz vaccine strain was generated in 1962 by additional passaging of the Edmonston strain in chick embryo fibroblasts [112]. The strain is produced by manufacturers in Europe and Brazil [113]. Moraten was also generated by additional passaging of the attenuated Edmonston-Enders virus in chick embryo fibroblasts [9] and it is used in the United States as Attenuvax, Merck & Co., [113]. Leningrad-4 was derived from an isolate obtained in 1957 in St Petersburg (formerly Leningrad), Russia [99]. Like Edmonston B, it proved to be insufficiently attenuated [114]. Further passaging led to the development of the Chinese vaccine strain Changchun-47 [115]. Shanghai-191 was developed from an isolate obtained in Shanghai in 1960 and attenuated through passages in human and avian cell culture systems [101]. It has been used continually since 1966 [98]. CAM-70 was derived from the Japanese wild-type isolate, Tanabe, by serial passaging in the chorioallantoic membrane of chickens [100], followed by passaging in chick embryo fibroblasts [116, 117]. CAM-70 is produced in Japan and Indonesia [113].

The first study comparing the full-length genomic sequences of the Edmonston-derived vaccine strains AIK-C, Moraten, Rubeovax, Schwarz, and Zagreb with the Edmonston wild-type strain was published in 2001 [95, 96]. It was followed by the sequences of independently derived CAM-70, Shanghai-191, and Changchun-47 [97, 98]. The sequence of Leningrad-4 was submitted to GenBank in 2004 by D. Zhao but was not published. Although the propagation of the Tanabe progenitor strain and the sequence of its H gene were reported recently [118], the remainder of the sequence of the genome of the Tanabe strain remains unavailable for comparison. The sequences of several vaccine strains that are still in use have not been determined yet. Among these are Leningrad-16, a vaccine strain derived from a Russian isolate [119, 120]; Schwarz F88, a Japanese vaccine derived by further passaging of the Schwarz strain [113]; and TD97, another Japanese vaccine that was generated from the Tanabe isolate [113].

COMPARATIVE SEQUENCE ANALYSIS

Phylogenetic Analysis

The total number of nucleotide changes compared with Edmonston wild-type is 29 for Leningrad-4; 33 for Zagreb; 36 for Rubeovax; 42 for AIK-C, Moraten, and Schwarz; 43 for Changchun-47; 50 for Shanghai-191; and 73 for CAM-70. Of the 3 viruses with the smallest number of substitutions, 2 (Leningrad-4 and Rubeovax) were insufficiently attenuated.